

# Supplemental Text

## 1 Introduction to mathematical model of bacterial growth

We discuss a mathematical model of bacterial growth. We use this model to address if the experimental results discussed in the main text and our rationale that the regulation of ribosome synthesis is non-optimal in response to DNA synthesis inhibitors can be reconciled with the paradigm of optimal regulation of ribosome synthesis under no stress conditions.

The model of bacterial growth describes the influx of resources into the cell and the consumption of these resources by the synthesis of proteins, ribosomes, and DNA. The model incorporates Cooper and Helmstetter’s classical results about chromosome replication and the cell division cycle of *Escherichia coli* [Cooper & Helmstetter, 1968] as well as Donachie’s “initiation mass” mechanism that couples protein synthesis to DNA replication [Donachie, 1968, Donachie & Blakely, 2003] and cell division. The model further captures optimal regulation of ribosome synthesis in different nutrient environments as a function of the intracellular level of resources like amino acids or ATP – a mechanism that is widely accepted as the means by which *E. coli* and other bacteria achieve maximal growth rates in different nutrient environments [Paul et al., 2004]. This regulatory mechanism based on the intracellular resource level applies to many bacterial species while the molecular details of its implementation vary from species to species. In a real cell a large number of different resources like NTPs, amino acids, folic acid, and others are consumed to synthesize DNA, proteins, ribosomes, and other cell components. In our model we simplify this complicated situation by introducing a single effective resource that is consumed in the synthesis of proteins, DNA, and ribosomes. While it does not correspond to any specific actual cellular resource, this effective resource is best thought of as a metabolic precursor that is shared by protein, DNA and RNA synthesis.

## 2 Kinetic equations

The following dynamical system describes the population averages of the amount of protein  $p$ , DNA  $c$ , ribosomes  $r$ , and resources  $a$  per cell in an exponentially growing bacterial culture. The variable  $p$  describes all protein in the cell except for ribosomal protein. Proteins, DNA, and ribosomes are synthesized by the cells and are diluted as a result of cell divisions. In addition, resources are consumed in the synthesis of these cell constituents:

$$\begin{aligned} dp/dt &= s_p - gp \\ dc/dt &= s_c - gc \\ dr/dt &= s_r - gr \\ da/dt &= s_a - (g + k_{\text{deg}})a - (\epsilon_p s_p + \epsilon_r s_r + \epsilon_c s_c) \end{aligned} \quad (1)$$

Here,  $g$  is the growth rate that leads to dilution of all components as a result of cell divisions and  $s_p$ ,  $s_c$ ,  $s_r$ , and  $s_a$  are the synthesis rates of ribosomes, proteins, DNA, and resources, respectively. These rates depend on the variables  $p$ ,  $c$ ,  $r$  and  $a$  (see below).  $\epsilon_p$ ,  $\epsilon_r$ , and  $\epsilon_c$  describe the amount of resources consumed to make one protein, ribosome, and chromosome, respectively. The resource degradation rate  $k_{\text{deg}}$  captures possible resource instability and resource turnover by processes that are not explicitly captured in the model. This rate  $k_{\text{deg}}$  could be set to zero without qualitatively changing the conclusions discussed here. In Eq. (1), we neglect protein degradation that only affects a small fraction of the total protein pool in *E. coli*.

Eq. (1) describes the mass and resource balance of the system. To fully define the theoretical description, we specify the synthesis rates  $s_p$ ,  $s_c$ ,  $s_r$ , and  $s_a$ :

$$\begin{aligned} s_p &= (1 - \eta) k_p^0 f_{\text{res}} \rho r \\ s_c &= N_f \times 1/(2\tau_C) \\ s_r &= N_{\text{rrn}} N_o \min(s_r^{\text{opt}}, s_r^0 f_{\text{res}}) \\ s_a &= \nu_a, \end{aligned} \quad (2)$$

with the functions

$$V = k_V (p + p_r r)$$

$$\begin{aligned}
\eta &= p_r s_r / (s_p + p_r s_r) \\
f_{\text{res}} &= \frac{a/V}{M_a + a/V} \\
N_o &= e^{g(\tau_D + \tau_C)} \\
N_f &= 2e^{g\tau_D} (-1 + e^{g\tau_C}) \\
1/\tau_C &= f_{\text{res}} \delta / \tau_C^0 \\
1/\tau_D &= f_{\text{res}} / \tau_D^0.
\end{aligned} \tag{3}$$

In the equation for  $s_p$  in (2),  $\eta$  is the fraction of ribosomes that translate ribosomal protein and  $k_p = k_p^0 f_{\text{res}}$  is the rate of protein synthesis per ribosome. The function  $f_{\text{res}}(a/V)$  describes the increase of the translation rate  $k_p$  as a function of the intracellular resource concentration  $a/V$ . For high resource concentrations, the translation rate saturates at the value  $k_p^0$ . Here, the cell volume  $V$  is proportional to the total amount of protein in the cell  $p + p_r r$  where  $p_r$  denotes the amount of ribosomal protein per ribosome. In agreement with previous studies, we assume that mRNA is always synthesized in sufficient amounts to provide all ribosomes with templates for protein synthesis so that a constant and large fraction of ribosomes (80 percent) are actively translating independent of environmental conditions [Bremer & Dennis, 1996]. Further,  $\rho$  is the fraction of ribosomes that are not blocked by a translation inhibitor, i.e.  $\rho = 1$  in absence of antibiotics.

In the equation for  $s_c$  in (2),  $N_f$  is the average number of replication forks per cell,  $\tau_C$  the average time it takes one replication fork to propagate from the replication origin to the terminus, and  $\tau_D$  the average delay time between completion of chromosome replication and cell division [Cooper & Helmstetter, 1968]. The average number of replication forks per cell  $N_f$  can be calculated from  $\tau_C$ ,  $\tau_D$ , and the growth rate  $g$  using the relation in Eq. (3) [Cooper & Helmstetter, 1968]. We assume that the rate of DNA synthesis  $1/\tau_C$  per pair of replication forks increases as a function of the intracellular resource concentration following  $f_{\text{res}}(a/V)$  and saturates at a maximal rate  $1/\tau_C^0$ . The parameter  $\delta$  with  $0 \leq \delta \leq 1$  describes a decrease of the DNA synthesis rate that results from the addition of a DNA synthesis inhibiting antibiotic. In the absence of antibiotics  $\delta = 1$ .

In general, the resource influx into the cell  $s_a$  depends on many factors like membrane proteins involved in nutrient uptake and metabolic processes that convert these nutrients into resources that are usable for protein, DNA, and RNA synthesis. For simplicity, we approximate this resource influx into the cell by a constant  $\nu_a$  that depends only on the nutrient availability in the environment (growth medium).

Finally, in the equation for  $s_r$  in (2),  $N_{\text{rrn}}$  is the number of *rrn* operons per chromosome ( $N_{\text{rrn}} = 7$  in the wild type strain),  $N_o$  is the average number of replication origins per cell [Bremer & Churchward, 1977], and  $s_r^0$  is the maximal possible ribosome synthesis rate per *rrn* operon. The definition of the function  $s_r^{\text{opt}}(a/V)$  that determines the regulation of ribosome synthesis as a function of the intracellular resource concentration  $a/V$  is discussed below. In brief, the equation in (2) means that in the absence of antibiotics,  $s_r$  is always regulated to the optimal value that ensures maximal growth in a given nutrient environment.

**Additional equation that determines the growth rate:** We are interested in steady state solutions of Eq. (1). A steady state solution with positive values of the variables  $p$ ,  $r$ ,  $c$ , and  $a$  exists for any growth rate  $g$  with  $g < k_p/p_r$ . The upper boundary of the growth rate  $k_p/p_r$  results from the fundamental limit where all ribosomes exclusively translate ribosomal protein. To constrain the value of  $g$  in the model, an additional equation is needed. We use

$$s_p = p_o g N_o. \tag{4}$$

This equation incorporates the mechanism first proposed by Donachie that couples protein synthesis to the initiation of DNA replication and cell division [Donachie, 1968]. In this mechanism, a new round of chromosome replication is initiated whenever the total protein content of the cell per origin of chromosome replication reaches a certain constant value. It follows directly from Eq. (4) that in steady state the amount of protein per replication origin  $p/N_o$  is constant and equal to  $p_o$ .

## 2.1 Optimal regulation of ribosome synthesis in different nutrient environments

Combining Eq. (1) with Eq. (4) yields a closed system of equations and enables us to calculate the optimal ribosome synthesis rate  $s_r$  that maximizes the growth rate  $g$  in different conditions. For  $\rho = \delta = 1$ , i.e. in the absence of antibiotics and for given  $\nu_a$ , we vary the value of  $s_r$  and determine the value  $s_r^{\text{max}}$  at which  $g$  is maximal in steady

state. We perform this calculation for a range of values of the nutrient influx  $\nu_a$  with  $\nu_a > 0$  to obtain a set of solutions that describes the effects of different nutrient environments (growth media). The maximal growth rate that can be achieved increases with increasing  $\nu_a$ . For realistic parameters (discussed in Section 3 below), the steady state cell composition at the optimal ribosome synthesis rate in different nutrient environments resulting from our model is in good agreement with experimentally observed values [Bremer & Dennis, 1996], see Figure S6. This agreement justifies our simplifying assumptions and shows that optimal regulation of ribosome synthesis can be incorporated in a model of bacterial growth in a way that is completely consistent with experimental data.

## 2.2 Effects of antibiotics

The set of solutions describing growth in the absence of antibiotics determines the optimal rate of ribosome synthesis per *rrn* operon  $s_r^{\text{opt}}$  as a function of the intracellular resource concentration  $a/V$ : It is defined as  $s_r^{\text{opt}}(a/V) = s_r^{\text{max}}/(N_{\text{rrn}}N_o)$ . Here, we approximate the average number of *rrn* operons per cell by  $N_{\text{rrn}}$  times the number of replication origins  $N_o$ . This is a good approximation because most of the *rrn* operons are located near the replication origin of the chromosome [Blattner et al., 1997]. Below, we will apply the function  $s_r^{\text{opt}}(a/V)$  to the case where antibiotics inhibit translation or DNA synthesis.

In presence of a DNA synthesis inhibitor, i.e. when  $\delta < 1$ , the growth rate can be limited by DNA synthesis which is not captured by Eq. (4). To account for this, we additionally use the equation

$$N_f = N_f^{\text{nd}}(g). \quad (5)$$

Here,  $N_f^{\text{nd}}(g)$  is the number of replication forks for the steady state solutions in absence of antibiotics in which  $g$  is varied by using different  $\nu_a$ . Eq. (5) ensures that the inhibition of DNA synthesis is not simply compensated by increasing the parallel replication of the chromosome using an increased number of replication forks; this would lead to a DNA content per cell that increases with increasing DNA synthesis inhibitor which is not observed experimentally [Georgopapadakou & Bertasso, 1991]. This could also be ensured by imposing other equations than (5) without changing the conclusions discussed here. For instance, one could assume that the number of replication forks  $N_f$  remains at the steady state value obtained for  $\delta = 1$  when  $\delta$  is reduced below 1. Eq. (5) determines the growth rate in conditions where the limiting factor that determines the growth rate is DNA synthesis and not protein synthesis as in the case described by Eq. (4). Both equations (4) and (5) implicitly define potentially different growth rates  $g$ . The actual growth rate is the minimum of the two values capturing that in presence of the different kinds of antibiotics growth is either limited by protein synthesis or by DNA synthesis while in absence of antibiotics, protein synthesis is the limiting factor for growth.

We apply the function  $s_r^{\text{opt}}(a/V)$  defined above to the case where antibiotics inhibit translation or DNA synthesis, i.e. where  $\rho < 1$  or  $\delta < 1$ . Figure 7 shows that this approach qualitatively captures changes in the total protein content per cell (Figure 7C), the up- and down-regulation of ribosome synthesis in response to the two different classes of antibiotics (Figure 7D), and the suppressive drug interactions observed between the two classes of antibiotics (Figure 7E). We define the magnitude of suppression in Figure 7E in analogy to the definition used in Figure 6D (Experimental Procedures). To apply this definition, a notion of drug concentration is required. The exact relations between the drug concentrations and the parameters  $\delta$  and  $\rho$  that describe the effects of these drugs are drug-specific and unknown. For simplicity, we thus assume that the DNA synthesis inhibitor concentration is proportional to  $1 - \delta$  and the translation inhibitor concentration to  $1 - \rho$ . Further, since the model does not capture changes in MIC, we use the line of 50 percent growth in the  $(1 - \delta)$ - $(1 - \rho)$  plane to quantify suppression.

## 2.3 Effects of gene deletions

We investigate the effects of the different genetically manipulated strains in the framework of our model.

***rrn* deletions:** Deleting one or several of the *rrn* operons corresponds to simply decreasing  $N_{\text{rrn}}$  below the wild type value ( $N_{\text{rrn}} = 7$ ) while leaving all other parameters unmodified. Figure 7B shows that these deletions lead to an increase in growth rate under DNA synthesis inhibition ( $\delta < 1$ ) but not in its absence. Further, six deletions ( $N_{\text{rrn}} = 1$ ) strongly decrease the magnitude of the suppressive drug interaction between DNA synthesis inhibitors and protein synthesis inhibitors (Figure 7E) as observed experimentally (Figure 6D).

***relA spoT* deletions:** Deleting the genes *relA* and *spoT* leads to over-expression of ribosomes resulting from the removal of guanosine tetraphosphate (ppGpp), a key negative regulator of ribosome synthesis. We capture this effect in the model by adding a small fraction  $\phi$  of the maximal possible ribosome synthesis rate  $s_r^0 f_{\text{res}}$  in a given condition to the optimal ribosome synthesis rate:  $s_r = N_o N_{\text{rtn}} \min(s_r^{\text{opt}}(a/V) + \phi s_r^0 f_{\text{res}}, s_r^0 f_{\text{res}})$ . Here,  $0 \leq \phi \leq 1$  describes the over-expression due to absence of ppGpp-dependent regulation. Figure 7E shows exemplarily for  $\phi = 0.4$  that the magnitude of the suppressive drug interaction between DNA synthesis inhibitors and protein synthesis inhibitors increases as a result of ribosome over-expression as observed experimentally (Figure 6B,C).

### 3 Parameter values

The parameters and variables of the model are listed in Table S3. Experimentally measured or inferred values for almost all parameters are available from the literature or online databases [Bremer & Dennis, 1996, Bionumbers, 2009]. Since  $a$  does not describe one specific resource for which the molecule number per cell could be measured, the value and scale (units) of this variable can be chosen arbitrarily. We choose the resource scale such that  $a = 1$  at 1 doubling/hour.

Using this choice of resource scale, we determine the values of  $\nu_a$ ,  $\epsilon_p$ ,  $\epsilon_r$ , and  $\epsilon_c$  from three constraints: (i) the ratios  $\epsilon_p/\epsilon_r$  and  $\epsilon_p/\epsilon_c$  of the parameters  $\epsilon_p$ ,  $\epsilon_r$ , and  $\epsilon_c$  that define the amount of resources consumed to synthesize protein, ribosomes, and DNA, respectively, correspond to those for the ATP turnover of these processes. (ii) At a reference growth rate  $g = 1$  doubling/hour, the amounts of ribosomes, proteins, and DNA per cell agree with the corresponding literature values [Bremer & Dennis, 1996]. (iii) The growth rate  $g$  must be maximal as a function of  $s_r$  with all other parameters fixed.

The parameter  $M_a$  that determines the resource concentration  $a/V$  at which  $f_{\text{res}}$  is at half maximum was chosen to give good agreement of  $f_{\text{res}}$  with the relative changes of the peptide and DNA chain elongation rates for different growth rates in different growth media [Bremer & Dennis, 1996], see Figure S6D. This is possible because for the steady state solutions obtained from varying  $\nu_a$  in absence of antibiotics,  $a/V$  increases with increasing  $g$ . Finally, a small value for the resource decay rate  $k_{\text{deg}}$  was chosen to capture possible resource instability and resource turnover by processes that are not captured in the model. This rate  $k_{\text{deg}}$  could be set to zero without qualitatively changing the conclusions discussed here.

### 4 Numerical solutions

We performed all numerical calculations using Mathematica 6.0 (Wolfram Research). In particular, steady state solutions of Eqs. (1), (4), and (5) were calculated by integrating the ordinary differential equations forward in time (using the NDSolve function) until a stable fixed point was reached. We verified that this solution does not depend on initial conditions in our numerical calculations. Suppression in the model was quantified from solutions in which  $\delta$  and  $\rho$  were varied on a  $17 \times 17$  two-dimensional lattice.

Symbol	Definition	Value	Source
$g$	Cell division rate, growth rate	$0.69\text{h}^{-1}$	-
$r$	Number of ribosomes per cell	$1.35 \times 10^4$	[Bremer & Dennis, 1996]
$p$	Number of proteins per cell	$2.4 \times 10^6$ †	[Bremer & Dennis, 1996]
$c$	Genome equivalents of DNA per cell	1.8	[Bremer & Dennis, 1996]
$a$	Number of resources per cell	1 *	-
$\eta$	Ribosomal protein fraction ( $0 < \eta < 1$ )	0.11	[Bremer & Dennis, 1996]
$k_p$	Rate of protein synthesis per ribosome	$0.038 \text{ s}^{-1}$ ◊, †	[Bremer & Dennis, 1996]
$\tau_C$	Replication time of chromosome, “C period”	50min	[Bremer & Dennis, 1996]
$\tau_D$	Delay before cell division, “D period”	25min ◊	[Bremer & Dennis, 1996]
$N_f$	Number of replication forks	2.1	[Bremer & Dennis, 1996]
$N_o$	Number of replication origins	2.4	[Bremer & Dennis, 1996]
$V$	Cell volume	$1\mu\text{m}^3$	[Bionumbers, 2009]
$\nu_a$	Resource influx	$2.42\text{h}^{-1}$	-
$k_{\text{deg}}$	Resource degradation rate	$0.12\text{h}^{-1}$	-
$\epsilon_p$	Resources consumed to make one protein	$8.1 \times 10^{-7}$ †, ‡	-
$\epsilon_r$	Resources consumed to make one ribosome	$2.2 \times 10^{-5}$ ‡	-
$\epsilon_c$	Resources consumed to make one chromosome	0.039 ‡	-
$M_a$	Resource conc. where chain elongation rates are at half max.	$0.53\mu\text{m}^{-3}$	-
$p_o$	Protein per replication origin [Donachie, 1968]	$9.9 \times 10^5$	Inferred
$p_r$	Amount of protein per ribosome	20.7†	[Bionumbers, 2009]
$k_V$	Cell volume per protein	$3.73 \times 10^{-7}\mu\text{m}^3$	Inferred
$k_p^0$	Maximal rate of protein synthesis per ribosome	$0.059 \text{ s}^{-1}$ †	Inferred
$s_r^0$	Maximal rate of ribosome synthesis per <i>rrn</i> operon	$72\text{min}^{-1}$	Inferred
$\tau_C^0$	Minimal replication time of chromosome	33min	Inferred
$\tau_D^0$	Minimal delay before cell division	16min ◊	Inferred
$N_{\text{rrn}}$	Number of <i>rrn</i> operons per chromosome	1 to 7	[Blattner et al., 1997]
$\rho$	Fraction of functional ribosomes ( $< 1$ with antibiotic)	0 to 1	-
$\delta$	Relative change of DNA synthesis rate ( $< 1$ with antibiotic)	0 to 1	-

Table S 3: Parameters and variables. Values above the horizontal line depend on the growth rate  $g$  and are shown for  $g = 1$  doubling/hour which, in the absence of antibiotics ( $\rho = \delta = 1$ ), occurs for a resource influx  $\nu_a = 2.42\text{h}^{-1}$ . Values for other growth rates which occur for different values of  $\nu_a$ ,  $\rho$ , and  $\delta$  are calculated using the values below the horizontal line, see text.

† assuming an average protein size of 360 amino acid residues

\* arbitrarily chosen (see text)

◊ based on ribosome efficiency 0.8 and chain elongation rate  $c_p$  from Table 3 in [Bremer & Dennis, 1996]

◊ for simplicity, we assume  $\tau_D = \tau_C/2$  which holds to a good approximation [Bremer & Dennis, 1996]

‡ the ratios of  $\epsilon_p$ ,  $\epsilon_r$ , and  $\epsilon_c$  correspond to the respective values for ATP molecule turnover to make an average protein, ribosome, and chromosome:  $\epsilon_p = 1500$ ,  $\epsilon_r = 4.02 \times 10^4$ ,  $\epsilon_c = 7.23 \times 10^7$  [Bionumbers, 2009]

## Supplemental Experimental Procedures

### Strain construction

In the ribosomal RNA deletion strains, each of the seven *rrn* operons was entirely deleted by the PCR allelic exchange method (Datsenko and Wanner, 2000) to give seven kanamycin marked *rrn* deletion strains. Deletions spanned the *rrn* promoters and terminators. Ribosomal RNA deletions were then combined into a strain with all *rrn* operons removed from the chromosome by a successive series of P1 transduction and kanamycin resolution steps with FLP resolvase (pCP20). A tRNA plasmid (ptRNA67) was introduced at the  $\Delta 5$  stage. Deletions were confirmed by PCR and Southern blots. All *rrn* deletion strains used in this study including the  $\Delta 6$  strain show little variation in morphology and form uniform colonies which is a sign of genetic stability.  $\Delta 4$  and  $\Delta 6$  strains with different remaining *rrn* operons show similar results in our key experiments (Figures S11 and S12) and the effects of *rrn* deletion can be partially revoked by genetic complementation (Figures S13, S14) indicating that random second site mutations that might have occurred in the construction of these strains do not significantly affect our results.

The  $\Delta relA$  and  $\Delta relA \Delta spoT$  strains are from (Traxler et al., 2008). For the  $\Delta relA \Delta spoT$  strain, we verified the absence of suppressor mutations in *rpoBC* and *rpoD* before and after our experiment (Figure S15) using a standard control that is based on the fact that these strains cannot grow on minimal medium (Xiao et al., 1991) while suppressor mutations in *rpoBC* and *rpoD* allow for growth on minimal medium (Barker et al., 2001; Bartlett et al., 1998; Hernandez and Cashel, 1995; Zhou and Jin, 1998). Strain specifications are given in Table S2.

### Chromosomal integration of promoter-GFP constructs

To verify that effects of reporter plasmid copy number changes on the measured expression level are independent of promoter, we integrated promoter-GFP constructs (*lexA*, *folA*, and *hisL*) into the *phoA* locus of strain TB10 (Johnson et al., 2004) by using  $\lambda$  Red-mediated recombination (Yu et al., 2000); we used primers

AAGAAGTTATTGAAGCATCCTCGTCAGTAAAAAGTTAATCTTTTCAACAGACC  
AGAACAGCCCGTTTGCG and

CAGCAAAAAAACCCAGCGGAGCGAAAATTCACTGCCGGGCGCGGTTTTAG  
GATCTATCAACAGGAGTCCAAGCG where the underlined sequence is

homologous to the integration site. We verified successful integration events by colony PCR. Integrated constructs were moved into MG1655 by P1 transduction. Measuring fluorescence intensity, we find that the ratio of GFP expressed from the plasmid to GFP expressed from the chromosome is  $\sim 5$  and increases as growth rate is decreased by adding antibiotics or changing carbon source, consistent with an increase in plasmid copy number. This increase is identical for the three promoters tested and is thus well corrected by normalization to the median expression level change.

## Supplemental Figure Legends

**Figure S1. Disappearance of suppression is incremental with number of *rrn* deletions and does not depend on growth medium, or the specific DNA synthesis or translation inhibitor used.** (A,B) Growth rates of WT and *rrn* deletion strains in a two-dimensional concentration gradient of DNA synthesis inhibitor TMP and translation inhibitor SPR in rich LB medium (A) and glucose M9 minimal medium (B). MIC line shown in magenta. (C,D) As A,B, using DNA synthesis inhibitor CPR and translation inhibitor TET. The suppressive drug interaction (WT) is reduced in magnitude and eventually disappears as ribosome synthesis is reduced ( $\Delta 4$ ,  $\Delta 5$ ,  $\Delta 6$ ). Small black dots, concentrations at which growth rate was sampled. For raw growth curve data, see Figures S8 and S9.

**Figure S2. Regulation of ribosomal promoters for the DNA synthesis inhibitors CPR and NAL.** (A) Normalized expression levels  $\varepsilon_x$  of 110 promoters in *E. coli* as a function of median growth rate in various concentrations of CPR (Experimental Procedures). Ribosomal promoters, orange squares; SOS response promoters, black triangles; *rmf* promoter, black crosses. Random scatter added to growth rate for visibility. (B) Cumulative distributions of normalized expression levels  $\varepsilon_x$  at single concentrations of CPR and NAL (normalized growth rate  $\sim 0.45$ ). Ribosomal promoters, orange; other promoters, gray.

**Figure S3. Regulation of ribosomal promoters in drug combination of DNA synthesis inhibitor and translation inhibitor.** (A) Normalized expression level  $\varepsilon_x$  of ribosomal promoters *rplY*, *rpmE*, *rrsA*, *rpsU* and the mean normalized expression level of all nine ribosomal promoters investigated here (Table S1) in a two-dimensional concentration matrix of TMP and SPR (Experimental Procedures). Small black dots, concentrations at which expression level was sampled. (B) Change in expression level  $\varepsilon_x(\text{SPR}) / \varepsilon_x(\text{SPR}=0)$  as a function of SPR concentration, at no TMP (TMP=0, grey), and at a fixed TMP concentration (TMP=0.34 MIC, magenta). Up-regulation requires higher SPR concentration in the presence of TMP. Error-bars in B for promoters *rplY*, *rpmE*, *rrsA*, *rpsU* were estimated from the standard deviation of replicate measurements done on different days (see Figure S17). Error-bars for the mean normalized expression level of all nine ribosomal promoters investigated here (rightmost panel) show the standard error of the mean.

**Figure S4. Increased growth rate and survival resulting from reduced ribosome synthesis is specific to DNA synthesis inhibitors.** (A-E) Normalized growth rates of strains with incremental deletions of *rrn* operons arranged in order of increasing ribosomal expression under different antibiotics. Growth rate increases with decreasing ribosome synthesis from WT levels, under DNA synthesis inhibitors CPR (A) and NAL (B). Growth rate is unaffected or decreases with decreasing ribosome synthesis for translation inhibitors SPR (C)

and TET (D) as well as nitrofurantoin NIT (E) which acts by multiple mechanisms. Lines, 4<sup>th</sup> order polynomial fits. (F) MICs of antibiotics for  $\Delta 6$  strain relative to WT strain. Error bars show the standard deviation of replicates or the concentration resolution of the MIC determination, whichever is larger. Cultures grown in rich medium (LB).

**Figure S5. Reduced ribosome synthesis leads to smaller cell size under DNA synthesis inhibitors at the same relative growth inhibition.** (A) DIC images of WT cells and cells with reduced ribosome synthesis ( $\Delta 6$ ) growing in presence of DNA synthesis inhibitor (NAL) at the same relative growth inhibition ( $g \sim 0.3$  which corresponds to absolute growth rate  $0.2\text{h}^{-1}$  for WT and  $0.1\text{h}^{-1}$  for  $\Delta 6$ ); scale bar,  $10\ \mu\text{m}$ . (B) Cumulative distribution of cell lengths. Cell size of  $\Delta 6$  (squares) is slightly larger than that of WT (circles) in the absence of drugs but smaller in the presence of DNA synthesis inhibitor (NAL) at the same relative growth inhibition. This cell size difference is similar or even more pronounced if size distributions of  $\Delta 6$  and WT are compared at the same absolute growth rate or at the same drug concentration.

**Figure S6. Mathematical model with optimal regulation of ribosome synthesis quantitatively reproduces the changes in cell composition and growth rate that occur in different nutrient environments.** Comparison of model results to experimental data as growth rate changes in different nutrient environments. Lines show model results, symbols experimental data (Bremer and Dennis, 1996). (A) Total protein per cell. (B) DNA per cell. (C) Fraction of total protein that is ribosomal protein. (D) Peptide chain elongation rate (translation rate per ribosome; circles) and DNA chain elongation rate (DNA synthesis rate per replication fork; squares).

**Figure S7. Suppression relative to that seen for WT is amplified for a  $\Delta relA$  strain to a similar extent as for a  $\Delta relA \Delta spoT$  strain.** Growth rates of WT (A),  $\Delta relA$  (B), and  $\Delta relA \Delta spoT$  (C) strain in two-dimensional concentration gradients of DNA synthesis inhibitor (TMP) and translation inhibitor (SPR); MIC line, magenta. The suppressive drug interaction (A) is amplified in the  $\Delta relA$  strain (B) and in the  $\Delta relA \Delta spoT$  strain (C). *relA* deletions impair the cell's capability to synthesize ppGpp while not completely removing it like *relA spoT* deletions (Xiao et al., 1991). Since  $\Delta relA$  strains are less associated with the rapid occurrence of suppressor mutations in *rpoBC* and *rpoD* that are known to occur in  $\Delta relA \Delta spoT$  strains (Barker et al., 2001; Bartlett et al., 1998; Hernandez and Cashel, 1995; Zhou and Jin, 1998), these results support that our conclusions are not affected by suppressor mutations. Small black dots, concentrations at which growth rate was sampled. Note that absolute TMP MICs for the  $\Delta relA$  and  $\Delta relA \Delta spoT$  strains are about two-fold lower than those of the WT. For raw growth curve data, see Figure S10. Cultures grown in rich medium (LB).

**Figure S8. Raw growth curves of WT and mutants with reduced ribosome synthesis in two-dimensional drug matrix of TMP and SPR.** (A) Comparison of growth curves of WT and  $\Delta 6$  strain in identical two-dimensional concentration gradients of TMP and SPR in rich LB medium (Experimental Procedures). Each small box shows  $\log(\text{OD}_{600})$  versus time, see magnified box on bottom left for scales. (B) As A, comparing WT and  $\Delta 5$  strain in glucose M9 minimal medium (Experimental Procedures). (C) Repeat of  $\Delta 6$  in A with higher drug concentration resolution and lower SPR concentrations to verify absence of suppression.

**Figure S9. Raw growth curves of WT and mutants with reduced ribosome synthesis in two-dimensional drug matrix of CPR and TET.** (A,B) Growth curves of WT (A) and  $\Delta 6$  strain (B) in identical two-dimensional concentration gradients of CPR and TET in glucose M9 minimal medium (Experimental Procedures). Each small box shows  $\log(\text{OD}_{600})$  versus time, see magnified box on bottom left for scales. (C,D) As A,B, in rich medium (LB).

**Figure S10. Raw growth curves of WT and mutants with impaired regulation of ribosome synthesis in two-dimensional drug matrix of TMP and SPR.** Growth curves of WT (A),  $\Delta relA$  strain (B), and  $\Delta relA \Delta spoT$  strain (C) in identical two-dimensional concentration gradients of TMP and SPR in rich LB medium. Each small box shows  $\log(\text{OD}_{600})$  versus time, see magnified box on bottom left for scales. The decrease in MIC for TMP in the  $\Delta relA \Delta spoT$  strain was verified in independent experiments with higher concentration resolution along the TMP axis.

**Figure S11. Deletions of different sets of 4 or 6 *rrn* operons have similar effects on growth rate in the absence and in the presence of DNA synthesis inhibitors.** (A) Optical density ( $\text{OD}_{600}$ ) as a function of time for wild type MG1655 (black), two different  $\Delta 4$  strains ( $\Delta rrnGBAD$ , dashed green line;  $\Delta rrnGADE$ , dotted green line), and two different  $\Delta 6$  strains ( $\Delta rrnGADEHB$ , dashed magenta line;  $\Delta rrnGADBHC$ , dotted magenta line) in the absence of antibiotics. (B) As A, in the presence of a fixed concentration of the DNA synthesis inhibitor CPR. Results are similar if NAL is used instead of CPR (not shown). Note that all  $\Delta 4$  and  $\Delta 6$  strains have increased MICs for CPR and NAL (not shown). These results show that the growth rate phenotypes of the *rrn* deletion strains we report are reproducible across differently constructed *rrn* deletion strains. Consequently, they are unlikely to be caused by second site mutations that could occur in the construction of these strains. Cultures grown in rich medium (LB).

**Figure S12. Deletions of different sets of 4 or 6 *rrn* operons have similar effects on suppressive drug interactions between DNA synthesis inhibitors and translation inhibitors.** (A) Normalized growth rates in a two-dimensional drug matrix of TMP and SPR for the wild type strain MG1655 (see Figure 6B). (B) As A, for two different  $\Delta 4$  strains as indicated. (C) As A, for two different  $\Delta 6$  strains as indicated. While there are small differences in the shape of the MIC line, both  $\Delta 4$  strains show a strongly reduced magnitude of the suppressive drug

interaction compared to WT and suppression is completely absent in both  $\Delta 6$  strains. These results demonstrate that the suppression phenotypes of the *rrn* deletion strains we observe are reproducible across differently constructed *rrn* deletion strains. Consequently they are unlikely to be caused by second site mutations that could occur in the construction of these strains. Cultures grown in rich medium (LB).

**Figure S13. Complementation with a plasmid-borne *rrn* operon partially reverses the effects of *rrn* deletions on growth rate, in the presence and absence of a DNA synthesis inhibitor.** (A) Optical density ( $OD_{600}$ ) as a function of time for wild type MG1655 (solid line), a  $\Delta 6$  strain ( $\Delta rrnGADEHB$ , dashed line) and the same  $\Delta 6$  strain with plasmid pKK3535 that carries an *rrnB* operon (dotted line) in the absence of antibiotics. (B) As A, in the presence of a fixed concentration of the DNA synthesis inhibitor NAL (near the MIC of the wild type). (C) As B, but at a higher concentration of NAL (slightly above the MIC of the wild type). Results are similar if CPR is used instead of NAL (not shown). (D-F) As A-C, but using a different  $\Delta 6$  strain ( $\Delta rrnGADBHC$ , dashed line) complemented with plasmid pK4-16 that carries an *rrnB* operon (dotted line). (G-J) As A-C, but using two different  $\Delta 4$  strains ( $\Delta rrnGADE$ , dashed black line;  $\Delta rrnGBAD$ , dashed gray line) complemented with plasmid pKK3535 (black and gray dotted lines). These results indicate that the observed effects of *rrn* deletions on growth rate in these different environments are mostly due to changes in the ribosome level and are not caused by second site mutations that could occur in the construction of these strains. Cultures grown in rich medium (LB).

**Figure S14. Addition of a plasmid-borne *rrn* operon to a  $\Delta 6$  strain partially restores the suppressive drug interaction between DNA synthesis inhibitors and translation inhibitors.** (A) Normalized growth rates in a two-dimensional drug matrix of TMP and SPR for wild type MG1655 as in Figure 6B. (B) As A, for a  $\Delta 6$  strain ( $\Delta rrnGADEHB$ ). (C) As B, for the same  $\Delta 6$  strain bearing plasmid pK4-16, which carries an *rrnB* operon. These results show that the effects of *rrn* deletions on the magnitude of the suppressive drug interactions between DNA synthesis inhibitors and translation inhibitors are mostly due to changes in the ribosome level and are not caused by potential second site mutations that could possibly occur in the construction of these strains. Cultures grown in rich medium (LB).

**Figure S15. Absence of growth of  $\Delta relA\Delta spoT$  strain on minimal media plates indicates absence of suppressor mutations in RNA polymerase genes in this strain.** Strains  $\Delta relA\Delta spoT$  and  $\Delta relA$  were taken from wells with different concentrations of TMP and SPR (see schematic on right; cf. Figure 6C) after growth for 24h in this two drug environment and streaked on LB plates (left column) and glucose M9 minimal media plates (not supplemented with amino acids, right column). WT MG1655 grown in the absence of antibiotics was streaked on all plates as a positive control. Samples were taken from the following environments: (A) no drug, (B) highest concentration of TMP alone with

visible growth after 24h ( $OD_{600} > 0.06$ ), (C) highest concentration of SPR alone with visible growth after 24h, (D) two-drug environment of TMP and SPR at highest overall TMP concentration with visible growth after 24h (see schematic on right). In all cases, the  $\Delta relA \Delta spoT$  strain grows on LB but does not grow on minimal medium (Xiao et al., 1991). This confirms that suppressor mutations in *rpoBC* and *rpoD*, which can arise quickly in  $\Delta relA \Delta spoT$  mutants (Barker et al., 2001; Bartlett et al., 1998; Hernandez and Cashel, 1995; Zhou and Jin, 1998), do not occur at an appreciable rate in the course of our experiment. Differences in colony densities reflect samples from wells with different degrees of growth. LB plates were incubated at 37°C for 24h, M9 plates for 48h to ensure detection of slowly growing colonies.

**Figure S16. A *relA spoT* deletion strain has an increased lag time while its steady state growth rate is only slightly reduced compared to WT.** Eight replicates of growth curves (optical density as a function of time) for both WT MG1655 (black lines) and the  $\Delta relA \Delta spoT$  mutant (gray lines) are shown. Green lines are curves representing exponential growth with the median growth rate of all replicates for the WT, and for the  $\Delta relA \Delta spoT$  strain. The shown values for the growth rates are median  $\pm$  standard deviation of replicates. Note that the  $\Delta relA \Delta spoT$  strain has a clearly increased lag time but only a slightly reduced steady state growth rate. Cultures grown in rich medium (LB).

**Figure S17. Day-to-day variability of gene expression measurements.** Black circles show the standard deviation of the expression level  $\gamma$  (see Figure 3A) from seven replicate measurements (done on different days) of the promoters shown in Table S1 plotted as a function of the average expression level  $\gamma$  of each promoter. The red line indicates the maximum standard deviation as a function of the expression level which is used to estimate the error-bars in Figures 4B and S3B. Replicate measurements were done in the absence of antibiotics.

## Supplemental Tables

**Table S1: Transcriptional promoter-GFP reporter strains used in this study.**

Promoter	Description
<i>ampC</i> *	Beta-lactamase/D-ala carboxypeptidase; penicillin resistance, penicillin-binding protein (PBP)
<i>amyA</i> *	cytoplasmic alpha-amylase
<i>argA</i> *	N-alpha-acetylglutamate synthase (amino-acid acetyltransferase) (1st module)
<i>argQ</i> *	arginine tRNA 2 (duplicate of argV,Y,Z)
<i>aroH</i> *	3-deoxy-D-arabinoheptulosonate-7-phosphate synthase (DAHP synthetase), tryptophan repressible
<i>aroL</i> *	shikimate kinase II
<i>asnA</i>	asparagine synthetase A
<i>aspC</i>	aspartate aminotransferase, PLP-dependent
<i>aspU</i>	aspartate tRNA 1 (duplicate of aspT,V)
<i>atpI</i> *	membrane-bound ATP synthase subunit, F1-F0-type proton-ATPase
<i>bacA</i> *	bacitracin resistance; possibly phosphorylates undecaprenol
<i>bioB</i> *	biotin synthetase (2nd module)
<i>bolA</i> *	activator of morphogenic pathway (BoIA family), important in general stress response
<i>brnQ</i> *	LIVCS family, branched chain amino acid transporter system II (LIV-II)
<i>btuB</i> *	outer membrane porin, transporter for vitamin B12/cobalamin, receptor for E colicins, and bacteriophage BF23 (1st module)
<i>chpR</i>	part of proteic killer gene system, suppressor of inhibitory function of ChpA
<i>clpP</i> *	proteolytic subunit of clpA-clpP ATP-dependent serine protease, heat shock protein F21.5
<i>cls</i>	cardiolipin synthase
<i>cmr</i>	MFS superfamily transporter, multidrug/chloramphenicol efflux transporter (1st module)
<i>cpsG</i> *	phosphomannomutase in colanic acid gene cluster
<i>cpxR</i> *	response regulator in two-component regulatory system with CpxA, regulates expression of protein folding and degrading factors (OmpR family) (1st module)
<i>creD</i> *	tolerance to colicin E2
<i>cspA</i> *	major cold shock protein 7.4, transcription antiterminator of hns,
<i>cspB</i> *	Qin prophage; cold shock protein; may regulate transcription
<i>cspD</i> *	similar to CspA but not cold shock induced, nucleic acid-binding domain
<i>cusR</i> *	response regulator in two-component regulatory system with CusS, transcriptional regulation of copper resistance (1st module)
<i>cyoA</i> *	cytochrome o ubiquinol oxidase subunit II
<i>cysB</i> *	transcriptional regulator for biosynthesis of L-cysteine (LysR family) (1st module)
<i>cysP</i> *	ABC superfamily (peri_bind) thiosulfate transport protein
<i>cysT</i> *	cysteine tRNA
<i>dacA</i> *	D-alanyl-D-alanine carboxypeptidase, penicillin-binding protein 5 (1st module)
<i>dgkA</i> *	diacylglycerol kinase
<i>dinG</i>	LexA regulated (SOS) repair enzyme (2nd module)
<i>dinJ</i> *	damage-inducible protein J
<i>dinP</i> *	DNA polymerase IV, devoid of proofreading, damage-inducible protein P (1st module)
<i>dnaK</i> *	chaperone Hsp70 in DNA biosynthesis/cell division (1st module)
<i>dnaX</i> *	DNA polymerase III, tau and gamma subunits; DNA elongation factor III (1st module)
<i>dps</i> *	stress response DNA-binding protein; starvation induced resistance to H2O2, ferritin-like

<i>edd</i> *	6-phosphogluconate dehydratase
<i>emrA</i> *	multidrug resistance secretion protein
<i>emrE</i> *	DLP12 prophage; MFP family auxillary multidrug transport protein, methylviologen and ethidium resistance
<i>emrR</i>	transcriptional repressor of for multidrug resistance pump (MarR family)
<i>evgA</i> *	response regulator (activator) in two-component regulatory system with EvgS, regulates multidrug resistance (LuxR/UhpA family)
<i>fabZ</i>	(3R)-hydroxymyristol acyl carrier protein dehydratase
<i>fadB</i> *	multifunctional multimodular FadB: 3-hydroxybutyryl-coa epimerase (EC 5.1.2.3); delta(3)-cis-delta(2)-trans-enoyl-coa-isomerase (EC 5.3.3.8); enoyl-coa-hydratase (4.2.1.17) (1st module)
<i>fecA</i> *	outer membrane porin, receptor for ferric citrate, in multi-component regulatory system with cytoplasmic FecI (sigma factor) and membrane bound FecR (1st module)
<i>fecI</i> *	sigma (19) factor of RNA polymerase, affected by FecR and outer membrane receptor FecA (TetR/ArcR family)
<i>fepA</i> *	outer membrane porin, receptor for ferric enterobactin (enterochelin) and colicins B and D (1st module)
<i>flgM</i>	anti-FliA (anti-sigma) factor; also known as RflB protein
<i>fliA</i> *	sigma F (sigma 28) factor of RNA polymerase, transcription of late flagellar genes (class 3a and 3b operons)
<i>folA</i> *	dihydrofolate reductase type I; trimethoprim resistance
<i>fsr</i> *	MFS family fosmidomycin transport protein (2nd module)
<i>ftsZ</i> *	tubulin-like GTP-binding protein and GTPase, forms circumferential ring in cell division
<i>galE</i> *	UDP-galactose 4-epimerase (1st module)
<i>glgS</i> *	glycogen biosynthesis, rpoS dependent
<i>glnU</i> *	glutamine tRNA 1 (duplicate of glnW)
<i>gltB</i> *	glutamate synthase, large subunit (2nd module)
<i>gltJ</i> *	ABC superfamily (membrane), glutamate/aspartate transporter
<i>glyA</i> *	serine hydroxymethyltransferase (2nd module)
<i>gnd</i> *	gluconate-6-phosphate dehydrogenase, decarboxylating (1st module)
<i>gyrB</i>	DNA gyrase, subunit B (type II topoisomerase) (1st module)
<i>hdeA</i> *	conserved protein
<i>hipB</i> *	transcriptional repressor which interacts with HipA
<i>hisL</i> *	his operon leader peptide
<i>hisQ</i> *	ABC superfamily (membrane) histidine and lysine/arginine/ornithine transport system
<i>hisS</i> *	histidine tRNA synthetase (operon includes yfgL, see D. Kahne, Science, 2001)
<i>hslJ</i>	Heat shock protein hslJ
<i>htpG</i> *	chaperone Hsp90, heat shock protein C 62.5
<i>htpX</i> *	Heat shock protein, integral membrane protein
<i>htrA</i> *	periplasmic serine protease Do, heat shock protein (2nd module)
<i>icdA</i> *	isocitrate dehydrogenase in e14 prophage, specific for NADP+ (2nd module)
<i>iciA</i> *	inhibitor of replication initiation, also transcriptional regulator of dnaA and argK (affects arginine transport) (LysR family)
<i>ilex</i> *	isoleucine tRNA 2
<i>ilvL</i> *	ilvGEDA operon leader peptide
<i>inaA</i> *	pH inducible protein involved in stress response, protein kinase-like
<i>lacZ</i> *	Beta-galactosidase, lac operon
<i>lexA</i> *	transcriptional repressor for SOS response (signal peptidase of LexA family)
<i>lpdA</i> *	dihydrolipoamide dehydrogenase, FAD/NAD(P)-binding ; component of 2-oxodehydrogenase and pyruvate complexes; L protein of glycine cleavage complex second part (2nd module)
<i>lysA</i> *	diaminopimelate decarboxylase, PLP-binding (2nd module)

<i>macA</i> *	putative membrane protein
<i>malZ</i> *	maltodextrin glucosidase (2nd module)
<i>marR</i> *	transcriptional repressor for antibiotic resistance and oxidative stress
<i>mazG</i> *	conserved protein
<i>mdtH</i> *	putative MFS superfamily transport protein
<i>menF</i>	isochorismate synthase (isochorismate hydroxymutase 2), menaquinone biosynthesis
<i>mesJ</i> *	cell cycle protein
<i>metA</i>	homoserine transsuccinylase
<i>metJ</i>	transcriptional repressor for methionine biosynthesis (MetJ family)
<i>minC</i> *	cell division inhibitor; activated MinC inhibits FtsZ ring formation
<i>mrcB</i> *	bifunctional multimodular MrcB: tglycosyl transferase of penicillin-binding protein 1b (2nd module)
<i>mscL</i> *	mechanosensitive channel
<i>msrA</i> *	peptide methionine sulfoxide reductase
<i>murA</i> *	UDP-N-acetylglucosamine 1-carboxyvinyltransferase
<i>murC</i> *	L-alanine adding enzyme, UDP-N-acetyl-muramate:alanine ligase (1st module)
<i>napF</i>	Fe-S ferredoxin-type protein: electron transfer
<i>nfnB</i> *	dihydropteridine reductase/oxygen-insensitive NAD(P)H nitroreductase
<i>nhaA</i> *	NhaA family of transport protein, Na <sup>+</sup> /H antiporter (1st module)
<i>nrfA</i> *	nitrite reductase periplasmic cytochrome c(552):
<i>nuoA</i> *	NADH dehydrogenase I chain A
<i>ompN</i> *	outer membrane protein N, non-specific porin (1st module)
<i>osmC</i> *	resistance protein, osmotically inducible
<i>pabC</i>	4-amino-4-deoxychorismate lyase (aminotransferase) (2nd module)
<i>pepQ</i>	proline dipeptidase (2nd module)
<i>pfkA</i>	6-phosphofructokinase I
<i>pgpB</i>	phosphatidylglycerophosphate phosphatase B
<i>pheL</i> *	leader peptide of chorismate mutase-P-prephenate dehydratase
<i>plsB</i> *	glycerolphosphate acyltransferase (2nd module)
<i>pmbA</i>	peptide maturation protein, maturation of antibiotic MccB17, see tld genes ?
<i>pmrD</i>	polymyxin resistance protein B
<i>polA</i> *	DNA polymerase I, 3' --> 5' polymerase, 5' --> 3' and 3' --> 5' exonuclease (1st module)
<i>polB</i> *	DNA polymerase II and and 3' --> 5' exonuclease
<i>priA</i> *	primosomal protein N' (= factor Y) directs replication fork assembly at D-loops, ATP-dependent (2nd module)
<i>priC</i> *	primosomal replication protein N''
<i>proB</i>	gamma-glutamate kinase
<i>psiF</i> *	induced by phosphate starvation
<i>ptsG</i> *	multimodular PtsG: PTS family enzyme IIC, glucose-specific (1st module)
<i>pykF</i> *	pyruvate kinase I (formerly F), fructose stimulated (2nd module)
<i>rbfA</i> *	ribosome-binding factor, role in processing of 10S rRNA
<i>recA</i> *	DNA strand exchange and recombination protein with protease and nuclease activity (1st module)
<i>recN</i> *	protein used in recombination and DNA repair (2nd module)
<i>ribA</i>	GTP cyclohydrolase II
<i>rmf</i> *	ribosome modulation factor (involved in dimerization of 70S ribosomes)
<i>rnhA</i> *	RNase HI, degrades RNA of DNA-RNA hybrids
<i>rob</i> *	transcriptional activator for resistance to antibiotics, organic solvents and heavy metals (AraC/XylS family) (right origin binding protein) (1st module)
<i>rpiA</i> *	ribosephosphate isomerase, constitutive

<i>rpIL*</i>	50S ribosomal subunit protein L7/L12
<i>rpIN*</i>	50S ribosomal subunit protein L14
<i>rpIT*</i>	50S ribosomal subunit protein L20, also posttranslational autoregulator
<i>rpIY*</i>	50S ribosomal subunit protein L25
<i>rpmB*</i>	50S ribosomal subunit protein L28
<i>rpmE*</i>	50S ribosomal subunit protein L31
<i>rpmI*</i>	50S ribosomal subunit protein A
<i>rpoD*</i>	sigma D (sigma 70) factor of RNA polymerase , major sigma factor during exponential growth (2nd module)
<i>rpoE</i>	sigma E (sigma 24 ) factor of RNA polymerase, response to periplasmic stress (TetR/ArcR family)
<i>rpoH*</i>	sigma H (sigma 32) factor of RNA polymerase; transcription of heat shock proteins induced by cytoplasmic stress
<i>rpoS*</i>	sigma S (sigma 38) factor of RNA polymerase, major sigma factor during stationary phase
<i>rpsA*</i>	30S ribosomal subunit protein S1 (3rd module)
<i>rpsB*</i>	30S ribosomal subunit protein S2
<i>rpsT*</i>	30S ribosomal subunit protein S20
<i>rpsU*</i>	30S ribosomal subunit protein S21
<i>rrlA*</i>	23S rRNA
<i>rrlB*</i>	23S rRNA
<i>rrsA*</i>	16S rRNA
<i>rsd*</i>	regulator of sigma D, has binding activity to the major sigma subunit of RNAP
<i>sbcB*</i>	exonuclease I, 3' --> 5' specific; deoxyribophosphodiesterase
<i>sbmA*</i>	ABC superfamily (membrane module of atp&memb) transporter (2nd module)
<i>sbmC*</i>	DNA gyrase inhibitor
<i>sdhC*</i>	succinate dehydrogenase , cytochrome b556
<i>serA*</i>	D-3-phosphoglycerate dehydrogenase
<i>serC*</i>	3-phosphoserine aminotransferase / phosphohydroxythreonine transaminase
<i>serU*</i>	serine tRNA 2
<i>slp*</i>	outer membrane protein, induced after carbon starvation
<i>smpA*</i>	small membrane protein A
<i>soxS*</i>	transcriptional activator of superoxide response regulon (AraC/XylS family)
<i>sspA*</i>	stringent starvation protein A, regulator of transcription
<i>sufI*</i>	suppressor of ftsI, putative periplasmic protein, cupredoxin-like
<i>thiC*</i>	5'-phosphoryl-5-aminoimidazole = 4-amino-5-hydroxymethyl-2-methylpyrimidine-P tol protein required for outer membrane integrity, uptake of group A colicins, C-terminal is coreceptor with F pilus for filamentous phages, role in translocation of filamentous phage DNA to cytoplasm (1st module)
<i>tolA*</i>	outer membrane channel; specific tolerance to colicin E1; segregation of daughter chromosomes, role in organic solvent tolerance
<i>tolC*</i>	outer membrane channel; specific tolerance to colicin E1; segregation of daughter chromosomes, role in organic solvent tolerance
<i>trpR*</i>	transcriptional repressor for tryptophan biosynthesis (TrpR family)
<i>ttdA*</i>	L-tartrate dehydratase
<i>tyrB*</i>	tyrosine aminotransferase , tyrosine repressible, PLP-dependent
<i>ugpA*</i>	ABC superfamily (membrane) sn-glycerol 3-phosphate transport protein
<i>umuD*</i>	component of DNA polymerase V , signal peptidase with UmuC
<i>uspA*</i>	universal stress protein A
<i>uvrA*</i>	UvrA with UvrBC is a DNA excision repair enzyme (2nd module)
<i>uvrC*</i>	UvrC with UvrAB is a DNA excision repair enzyme (1st module)
<i>uvrD*</i>	DNA-dependent ATPase I and helicase II (1st module)
<i>wrbA*</i>	flavodoxin-like protein, trp repressor binding protein
<i>xseA</i>	exonuclease VII, large subunit

<i>yaeL</i> *	putative protease
<i>yajR</i> *	putative MFS family transport protein (1st module)
<i>yceE</i> *	putative MFS family transport protein (1st module)
<i>yddA</i> *	bifunctional multimodular YddA: putative ABC superfamily (membrane) transport protein (1st module)
<i>ydeA</i> *	MFS family, L-arabinose/isopropyl-beta-D-thiogalactopyranoside export protein, contributes to control of arabinose regulon (2nd module)
<i>ydeB</i> *	inner membrane protein involved in multiple antibiotic resistance
<i>ydhE</i> *	putative MATE family transport protein (1st module)
<i>ydiM</i> *	putative MFS family transport protein (1st module)
<i>yebG</i> *	DNA damage-inducible gene in SOS regulon, dependent on cyclic AMP and H-NS
<i>yebQ</i> *	putative MFS family transport protein (1st module)
<i>yjcR</i> *	putative multidrug resistance efflux pump protein, membrane protein
<i>ynfM</i>	putative MFS family transport protein (1st module)
<i>yojH</i> *	NA
<i>yojI</i> *	putative ABC superfamily (atp module of atp&membrane) transport protein (2nd module)

\* Promoters with low GFP signal. These were excluded from the analysis shown in Figure 3.

\* Promoters used for the two-dimensional drug concentration gradient of Figure 4.

**Table S2: Strains used in this study.**

Strain	Type	Source
WT	MG1655	-
WT (reporter strains)	MG1655 / pUA66 or pUA139	(Zaslaver et al., 2006)
Δ1	MG1655 <i>ΔrrnE</i>	This study (S. Quan)
Δ2	MG1655 <i>ΔrrnGB</i>	This study (S. Quan)
Δ3	MG1655 <i>ΔrrnGBA</i>	This study (S. Quan)
Δ4 <sup>♦</sup>	MG1655 <i>ΔrrnGADE</i>	This study (S. Quan)
Δ4	MG1655 <i>ΔrrnGBAD</i>	This study (S. Quan)
Δ5	MG1655 <i>ΔrrnGADEH</i> / ptRNA67	This study (S. Quan)
Δ6 <sup>♦</sup>	MG1655 <i>ΔrrnGADBHC</i> / ptRNA67	This study (S. Quan)
Δ6	MG1655 <i>ΔrrnGADEHB</i> / ptRNA67	This study (S. Quan)
<i>ΔrelA ΔspoT</i>	MG1655 <i>ΔrelA ΔspoT</i>	(Traxler et al., 2008)
<i>ΔrelA</i>	MG1655 <i>ΔrelA</i>	(Traxler et al., 2008)

<sup>♦</sup> Assay strain used unless otherwise indicated.

## Supplemental References

Barker, M. M., Gaal, T., and Gourse, R. L. (2001). Mechanism of regulation of transcription initiation by ppGpp. II. Models for positive control based on properties of RNAP mutants and competition for RNAP. *J Mol Biol* 305, 689-702.

Bartlett, M. S., Gaal, T., Ross, W., and Gourse, R. L. (1998). RNA polymerase mutants that destabilize RNA polymerase-promoter complexes alter NTP-sensing by *rrn* P1 promoters. *J Mol Biol* 279, 331-345.

Bionumbers (2009). <http://bionumbers.hms.harvard.edu/>.

Blattner, F. R., Plunkett, G., 3rd, Bloch, C. A., Perna, N. T., Burland, V., Riley, M., Collado-Vides, J., Glasner, J. D., Rode, C. K., Mayhew, G. F., *et al.* (1997). The complete genome sequence of *Escherichia coli* K-12. *Science* 277, 1453-1474.

Bremer, H., and Churchward, G. (1977). An examination of the Cooper-Helmstetter theory of DNA replication in bacteria and its underlying assumptions. *J Theor Biol* 69, 645-654.

Bremer, H., and Dennis, P. P. (1996). Modulation of Chemical Composition and Other Parameters of the Cell by Growth Rate, In *Escherichia coli* and *Salmonella*, F. C. Neidhardt, ed. (Washington, D.C.: ASM Press), pp. 1553-1569.

Cooper, S., and Helmstetter, C. E. (1968). Chromosome replication and the division cycle of *Escherichia coli* B/r. *J Mol Biol* 31, 519-540.

Datsenko, K. A., and Wanner, B. L. (2000). One-step inactivation of chromosomal genes in *Escherichia coli* K-12 using PCR products. *Proc Natl Acad Sci U S A* 97, 6640-6645.

Donachie, W. D. (1968). Relationship between cell size and time of initiation of DNA replication. *Nature* 219, 1077-1079.

Donachie, W. D., and Blakely, G. W. (2003). Coupling the initiation of chromosome replication to cell size in *Escherichia coli*. *Curr Opin Microbiol* 6, 146-150.

Georgopapadakou, N. H., and Bertasso, A. (1991). Effects of quinolones on nucleoid segregation in *Escherichia coli*. *Antimicrob Agents Chemother* 35, 2645-2648.

Hernandez, V. J., and Cashel, M. (1995). Changes in conserved region 3 of *Escherichia coli* sigma 70 mediate ppGpp-dependent functions in vivo. *J Mol Biol* 252, 536-549.

Johnson, J. E., Lackner, L. L., Hale, C. A., and de Boer, P. A. (2004). ZipA is required for targeting of DMinC/DicB, but not DMinC/MinD, complexes to septal ring assemblies in *Escherichia coli*. *J Bacteriol* 186, 2418-2429.

Paul, B. J., Ross, W., Gaal, T., and Gourse, R. L. (2004). rRNA transcription in *Escherichia coli*. *Annu Rev Genet* 38, 749-770.

Traxler, M. F., Summers, S. M., Nguyen, H. T., Zacharia, V. M., Hightower, G. A., Smith, J. T., and Conway, T. (2008). The global, ppGpp-mediated stringent response to amino acid starvation in *Escherichia coli*. *Mol Microbiol* 68, 1128-1148.

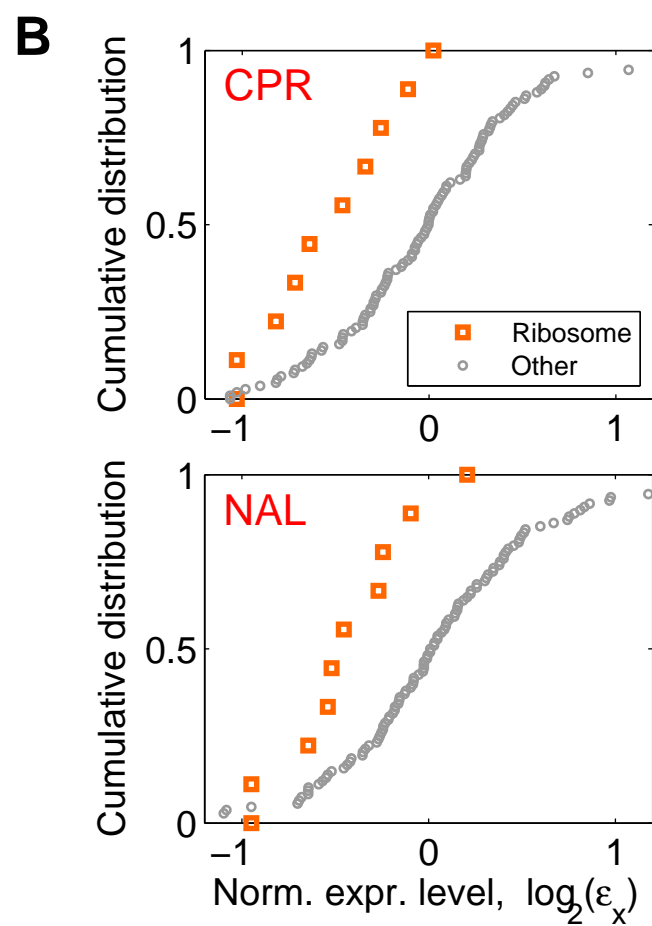
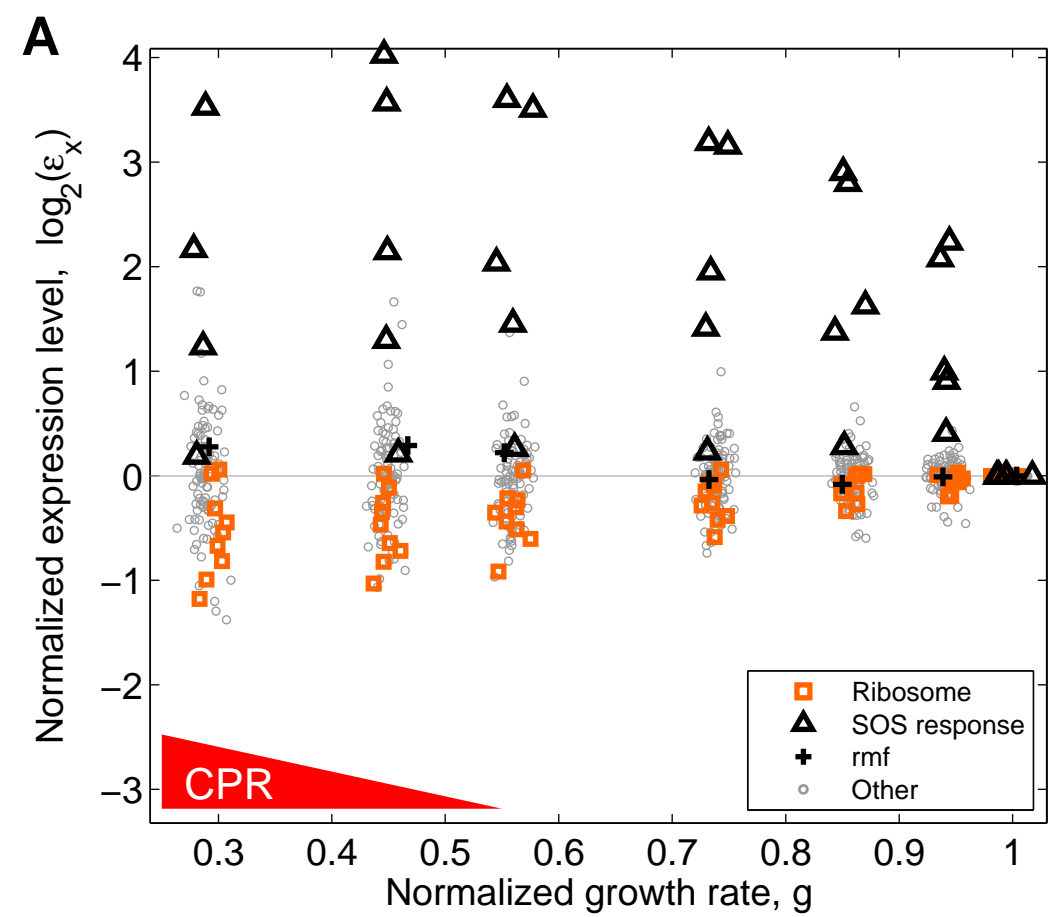
Xiao, H., Kalman, M., Ikehara, K., Zemel, S., Glaser, G., and Cashel, M. (1991). Residual guanosine 3',5'-bispyrophosphate synthetic activity of *relA* null mutants can be eliminated by *spoT* null mutations. *J Biol Chem* 266, 5980-5990.

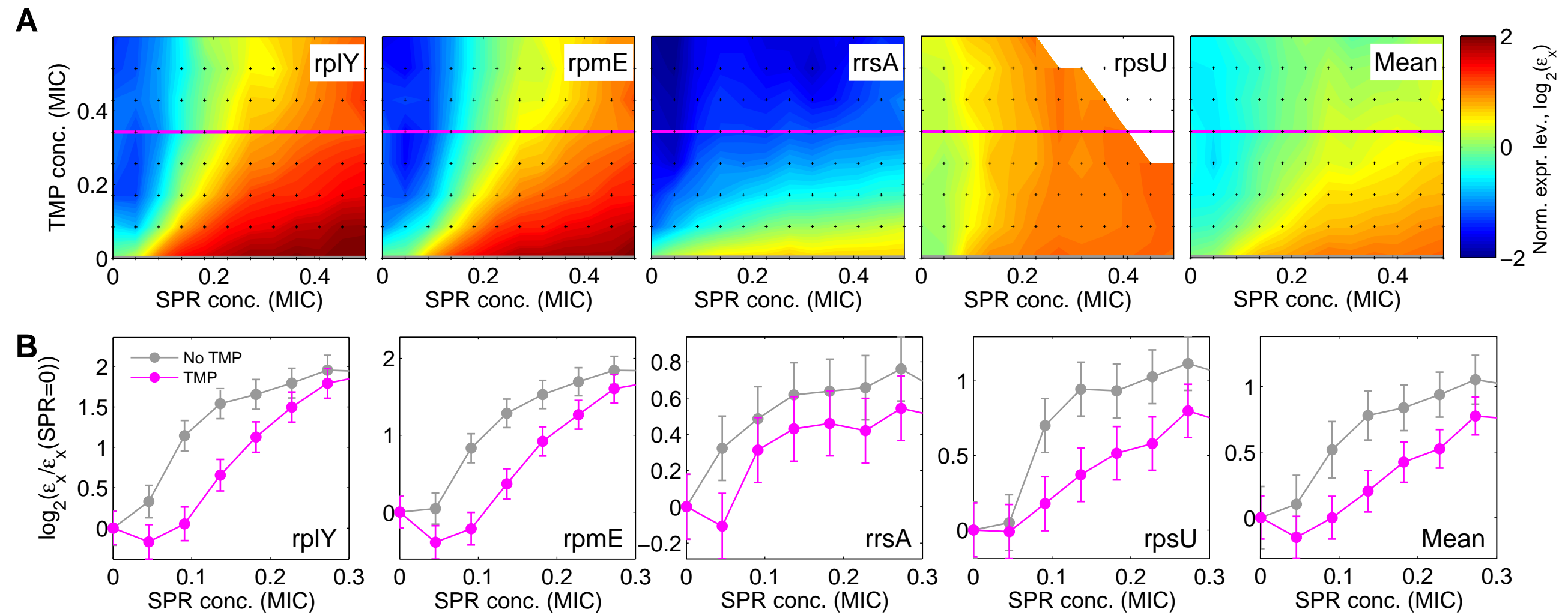
Yu, D., Ellis, H. M., Lee, E. C., Jenkins, N. A., Copeland, N. G., and Court, D. L. (2000). An efficient recombination system for chromosome engineering in *Escherichia coli*. *Proc Natl Acad Sci U S A* 97, 5978-5983.

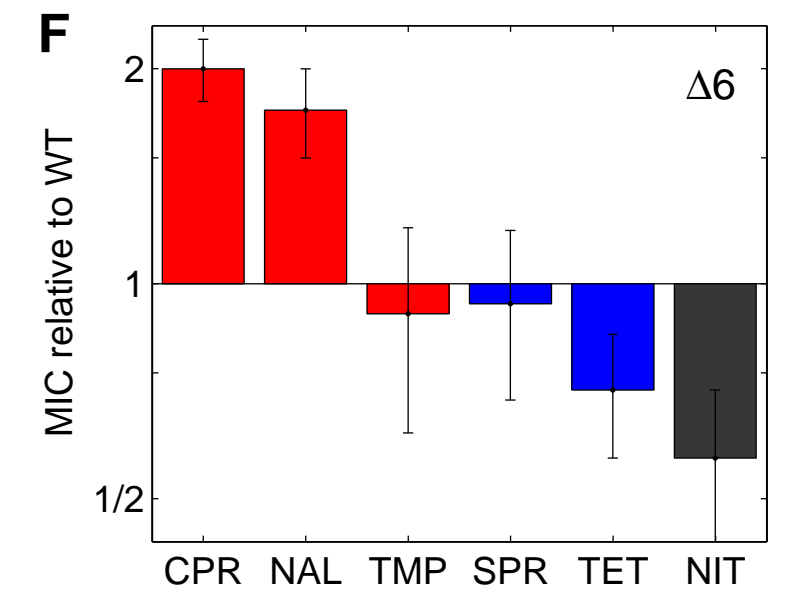
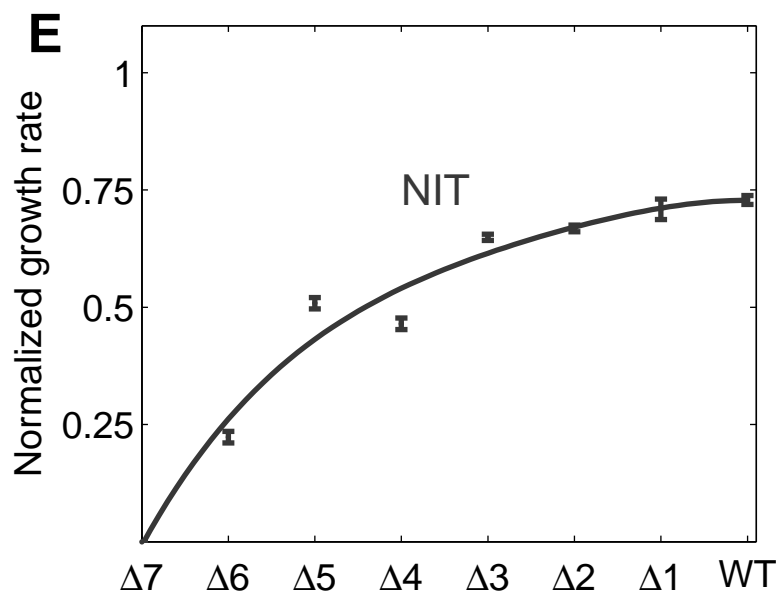
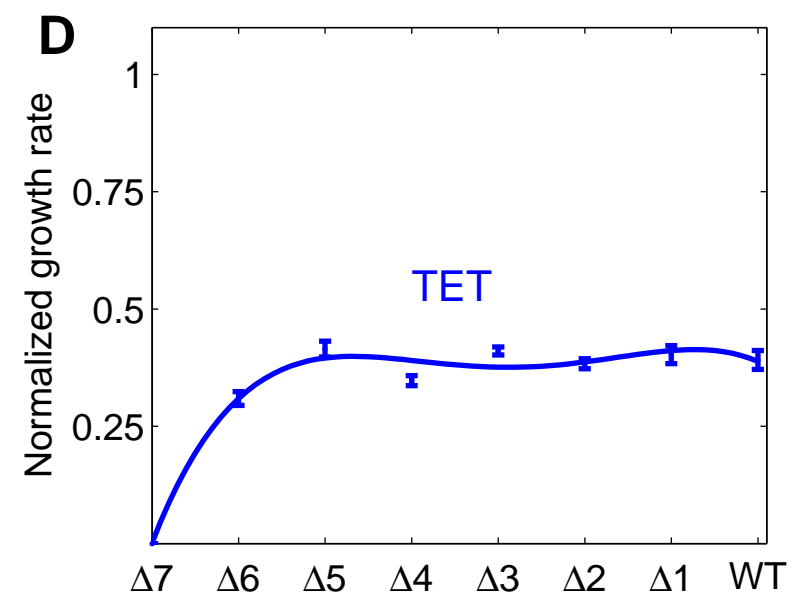
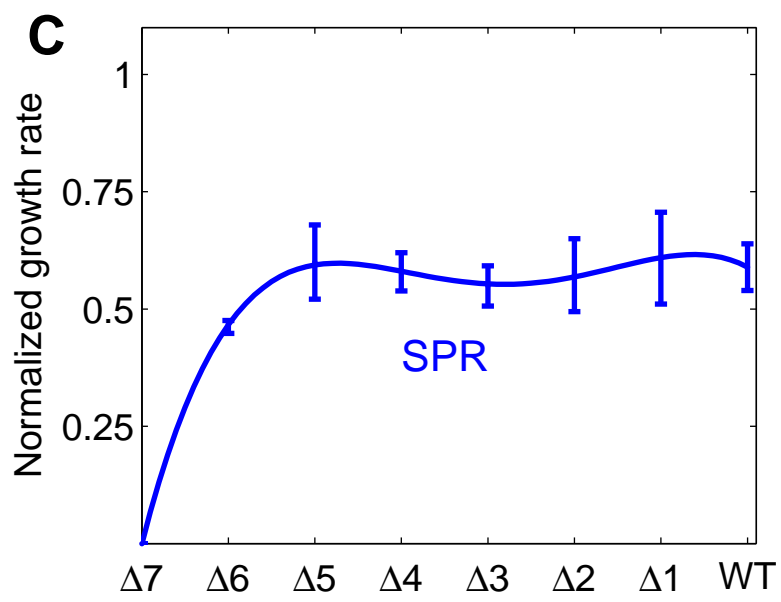
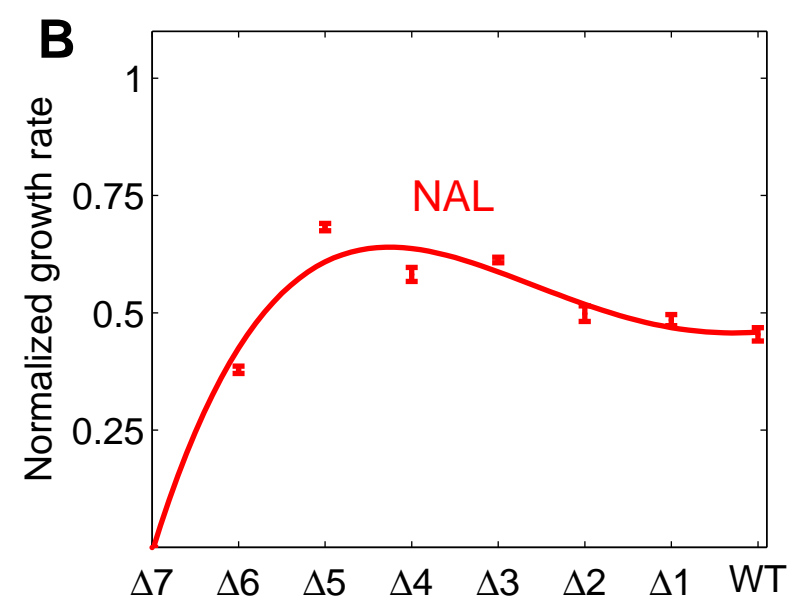
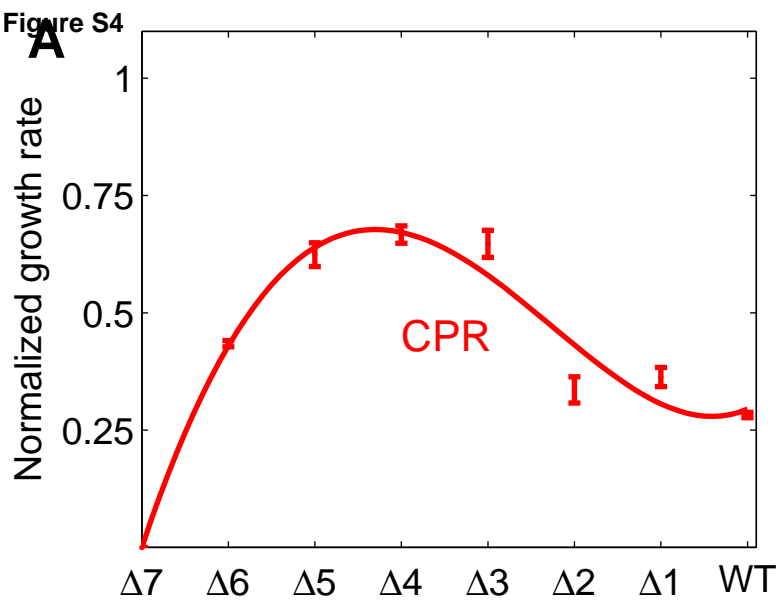
Zaslaver, A., Bren, A., Ronen, M., Itzkovitz, S., Kikoin, I., Shavit, S., Liebermeister, W., Surette, M. G., and Alon, U. (2006). A comprehensive library of fluorescent transcriptional reporters for *Escherichia coli*. *Nat Methods* 3, 623-628.

Zhou, Y. N., and Jin, D. J. (1998). The *rpoB* mutants destabilizing initiation complexes at stringently controlled promoters behave like "stringent" RNA polymerases in *Escherichia coli*. *Proc Natl Acad Sci U S A* 95, 2908-2913.

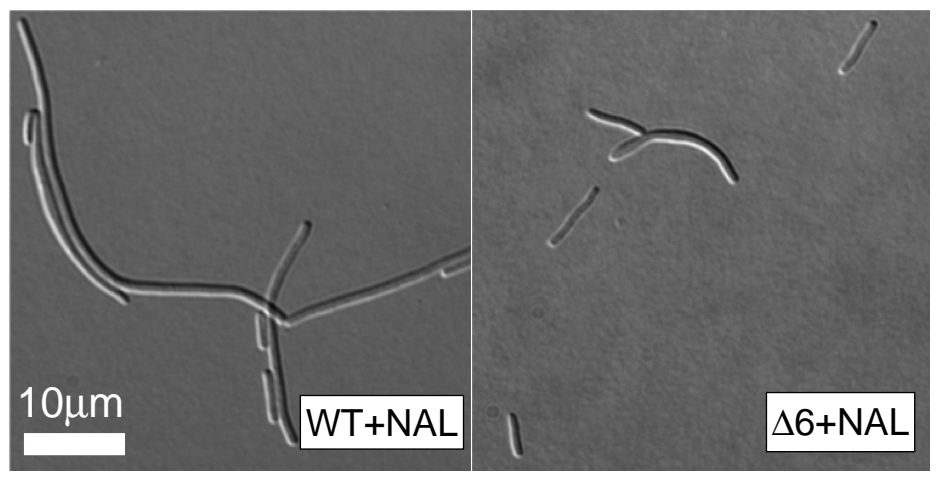




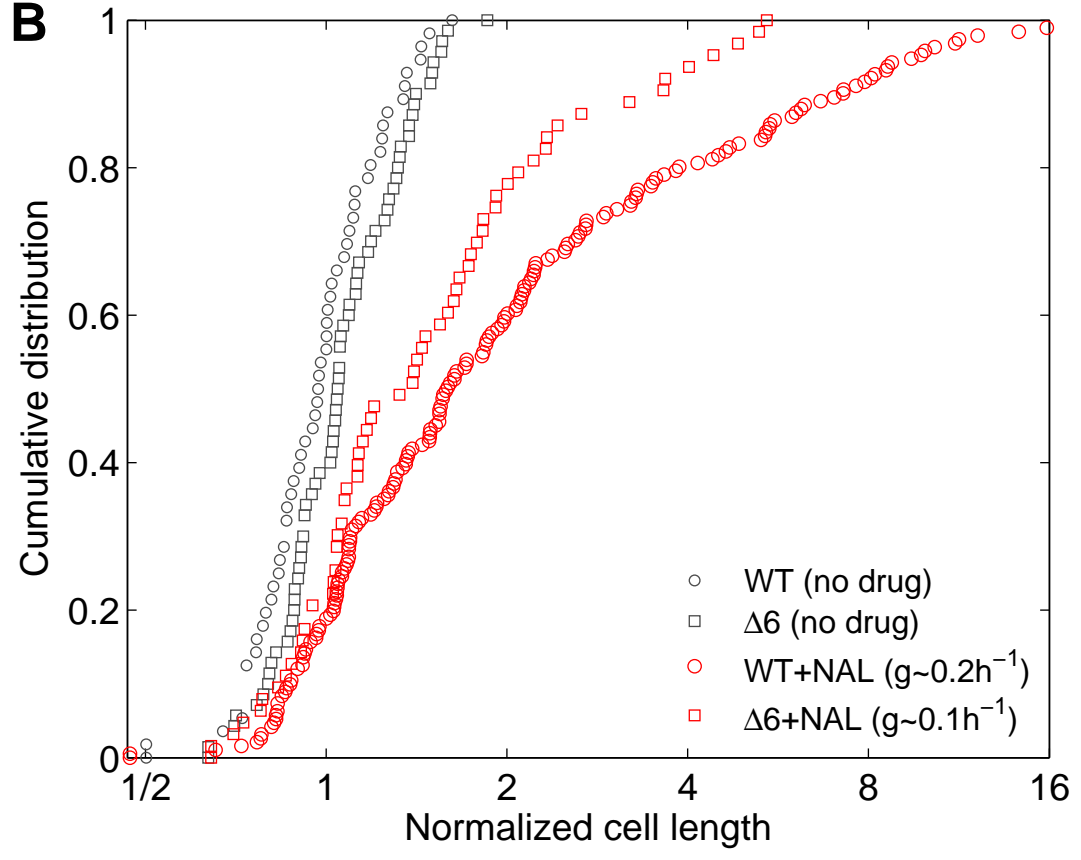


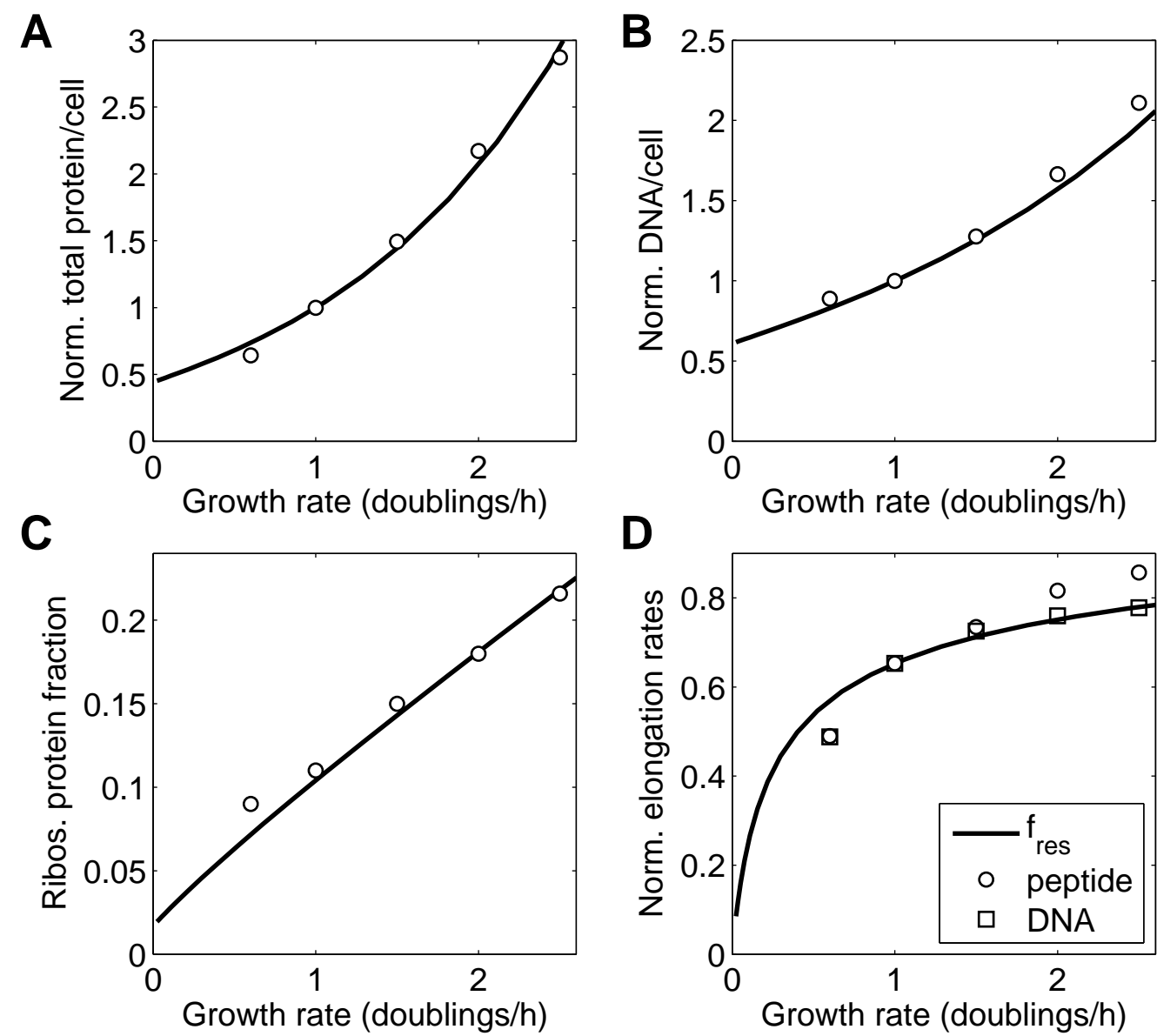


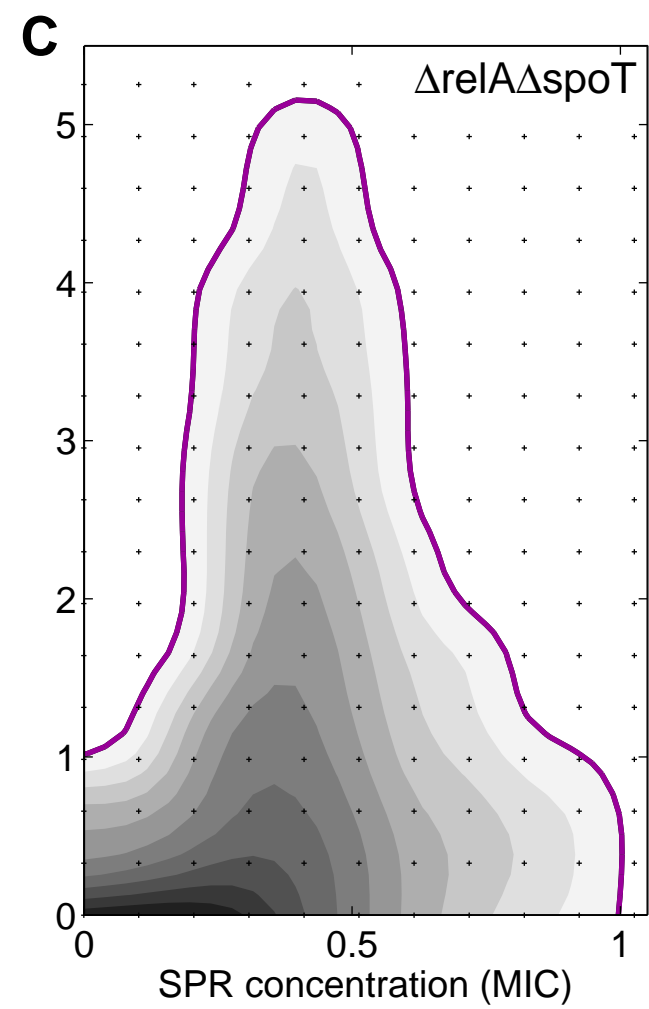
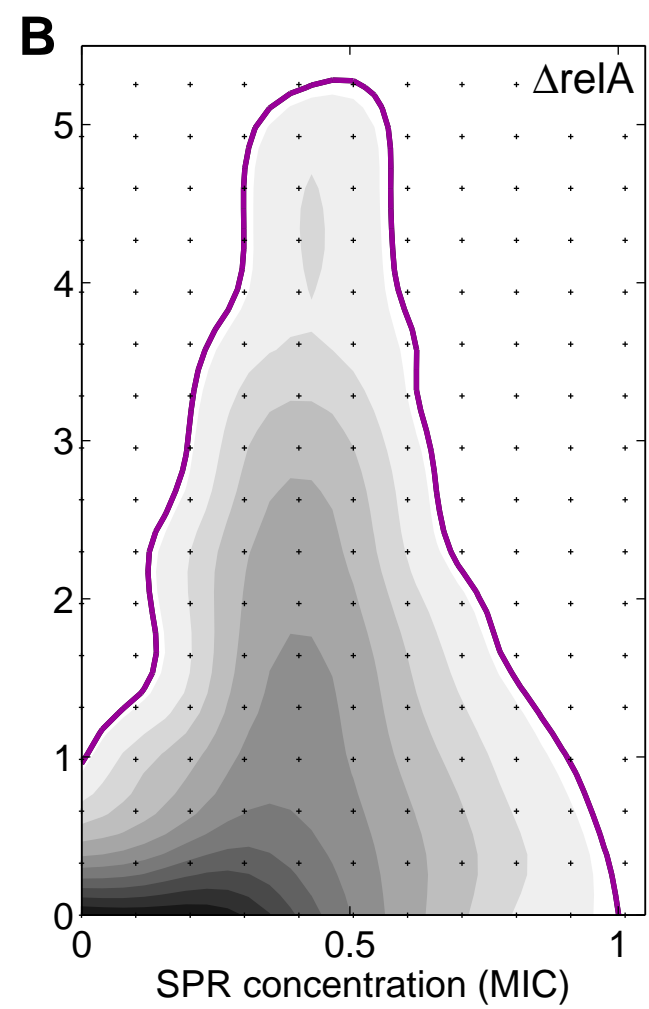
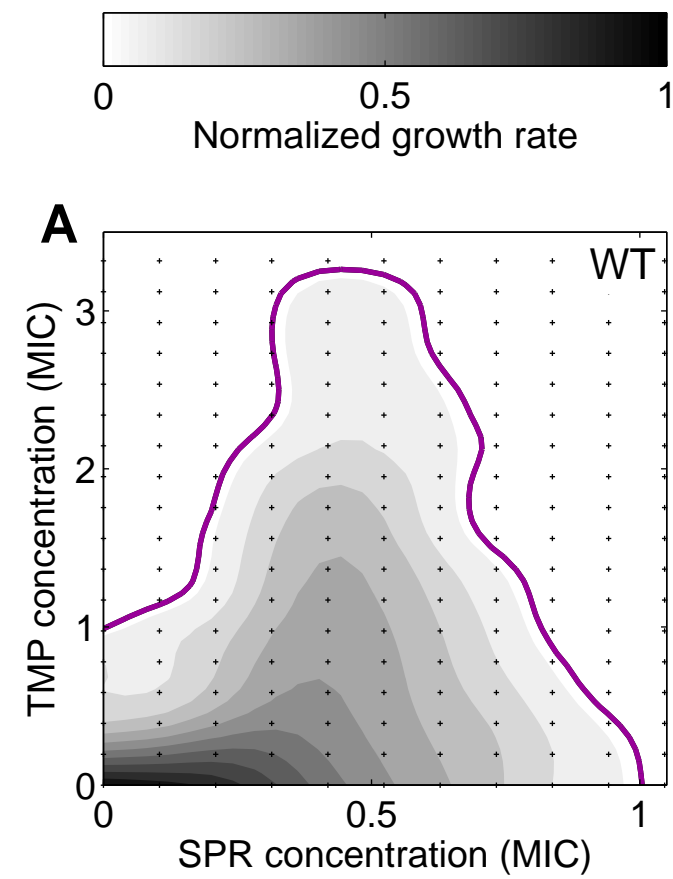
**A**



**B**







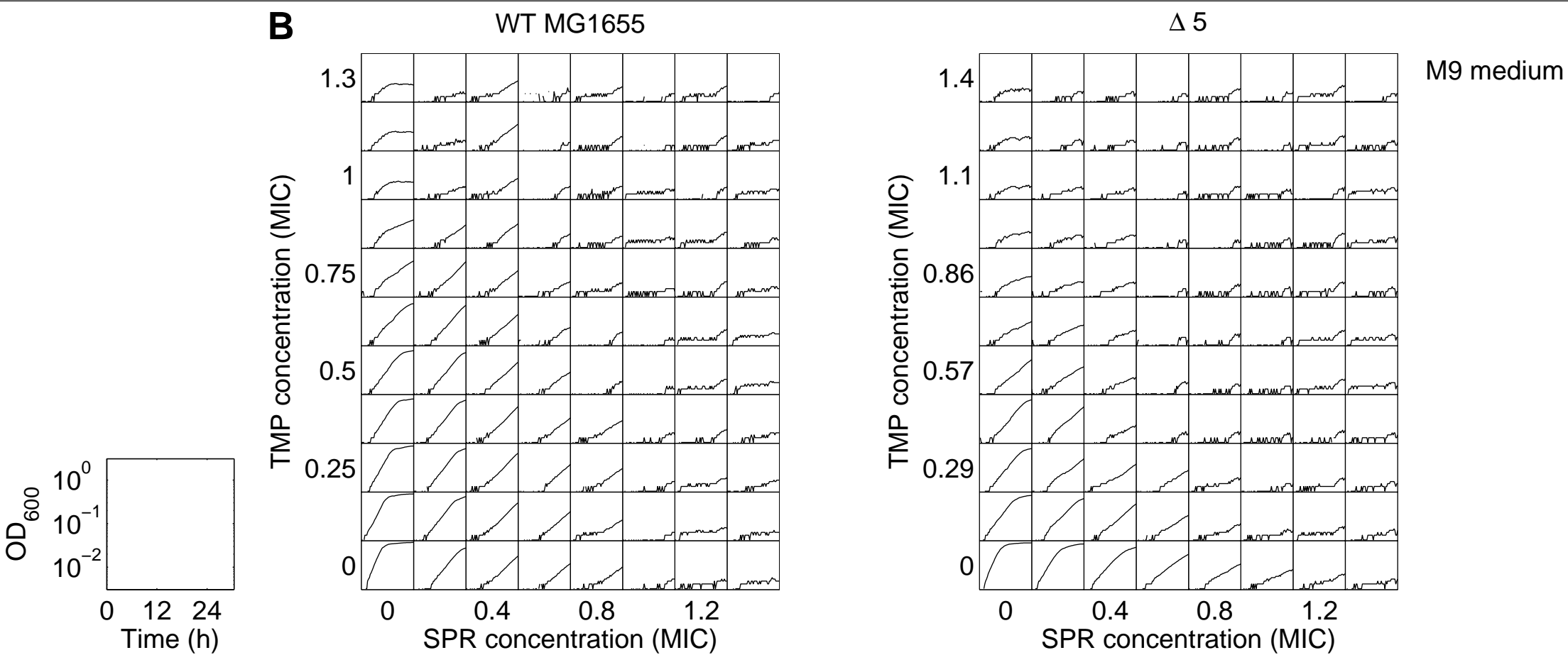
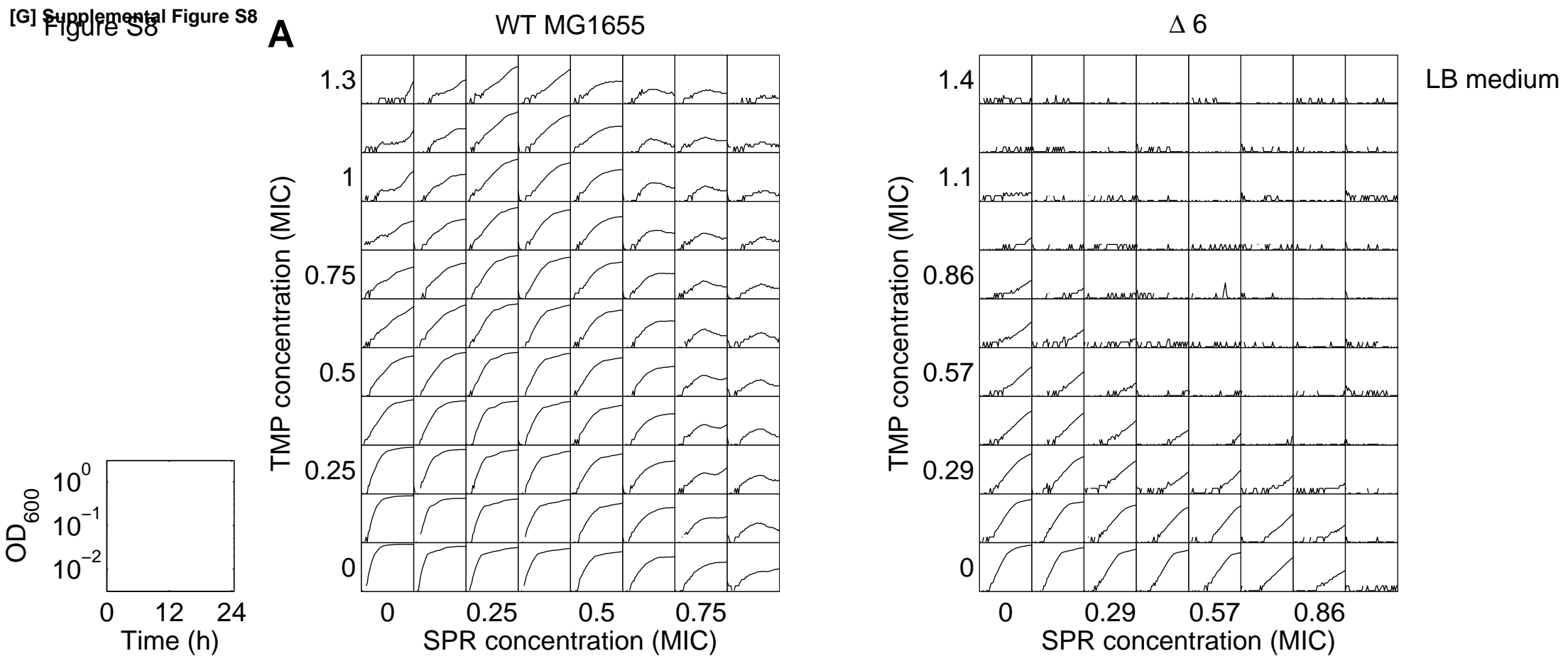
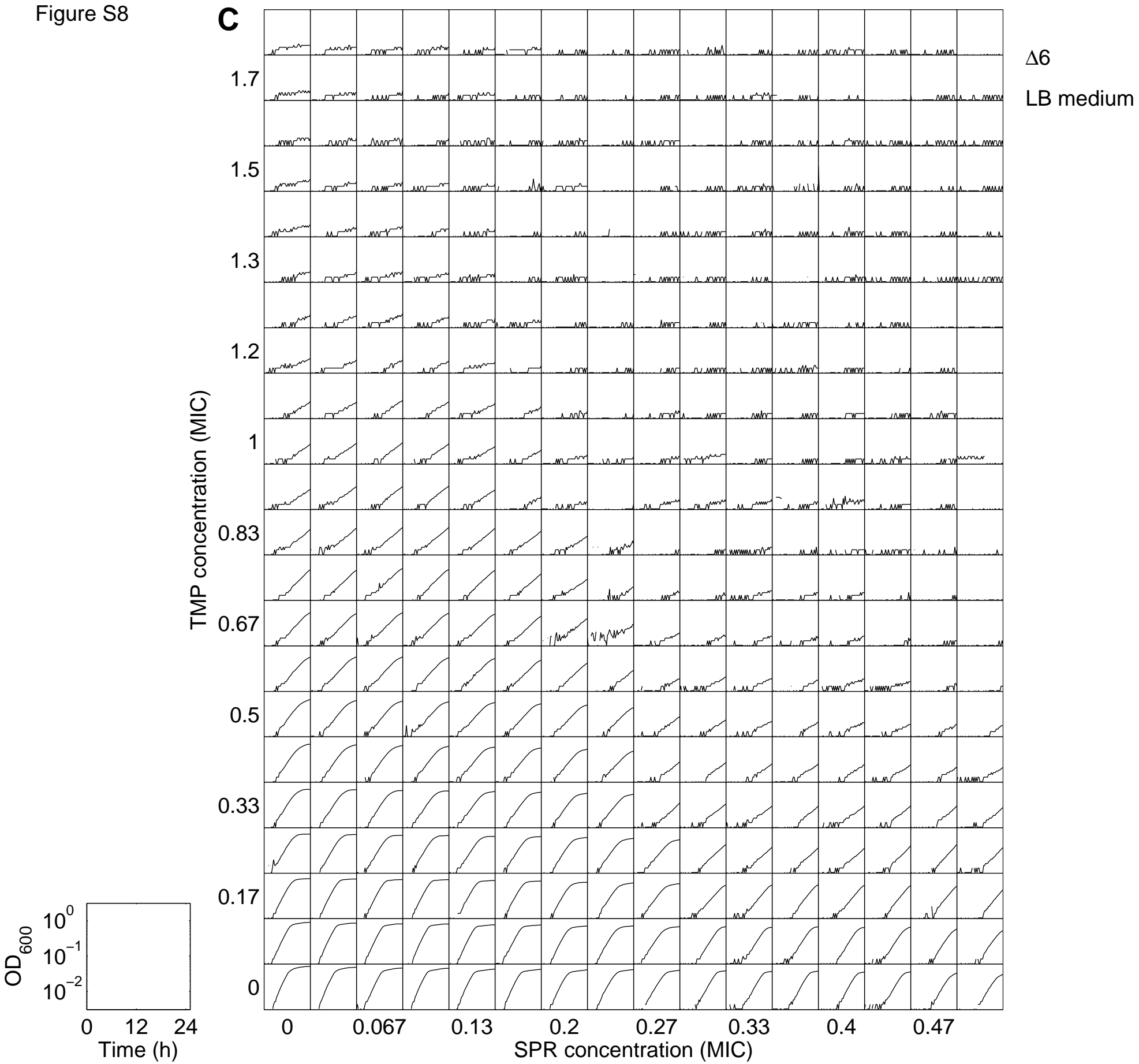


Figure S8



**A**

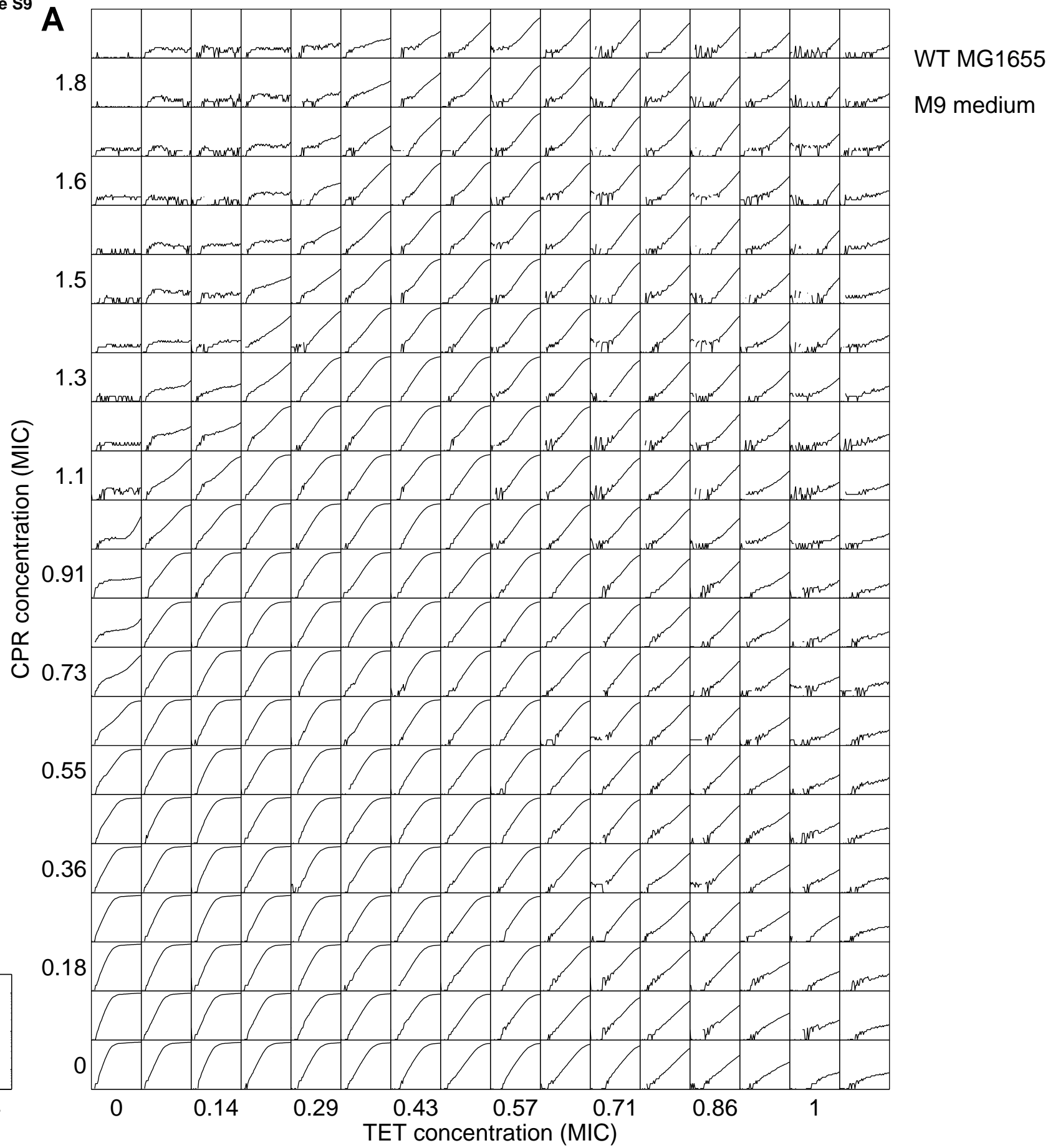


Figure S9

**B**

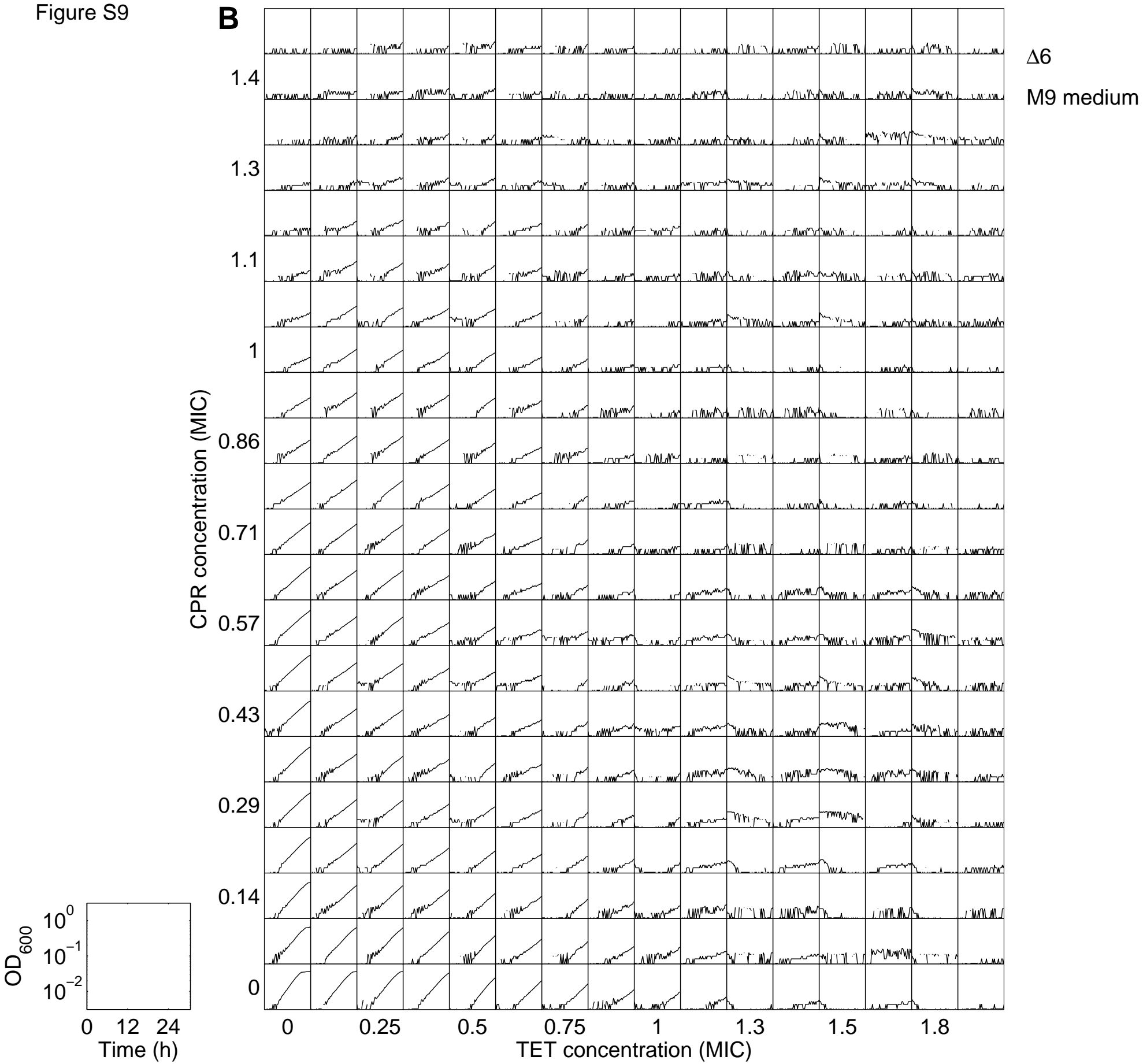


Figure S9

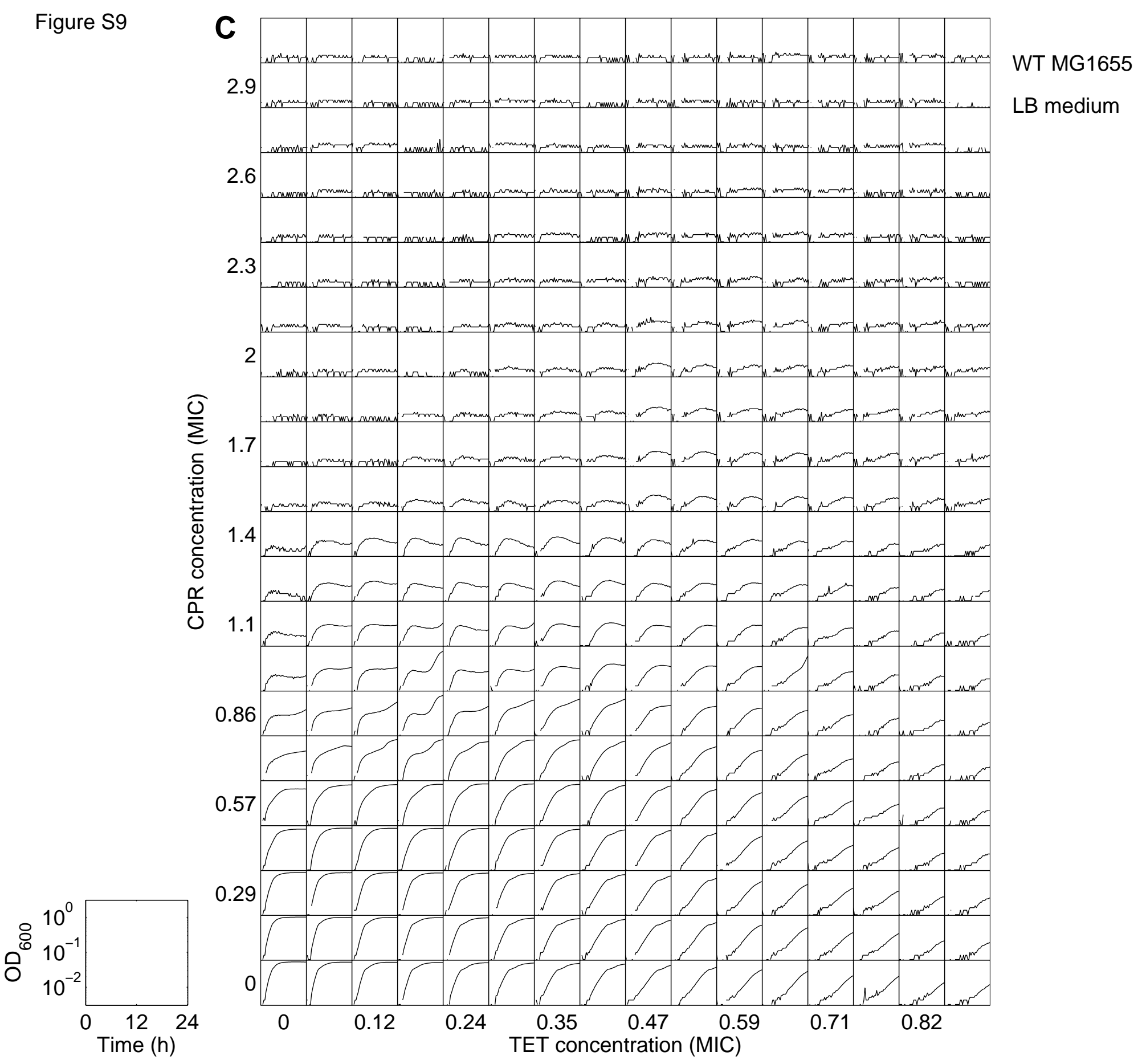
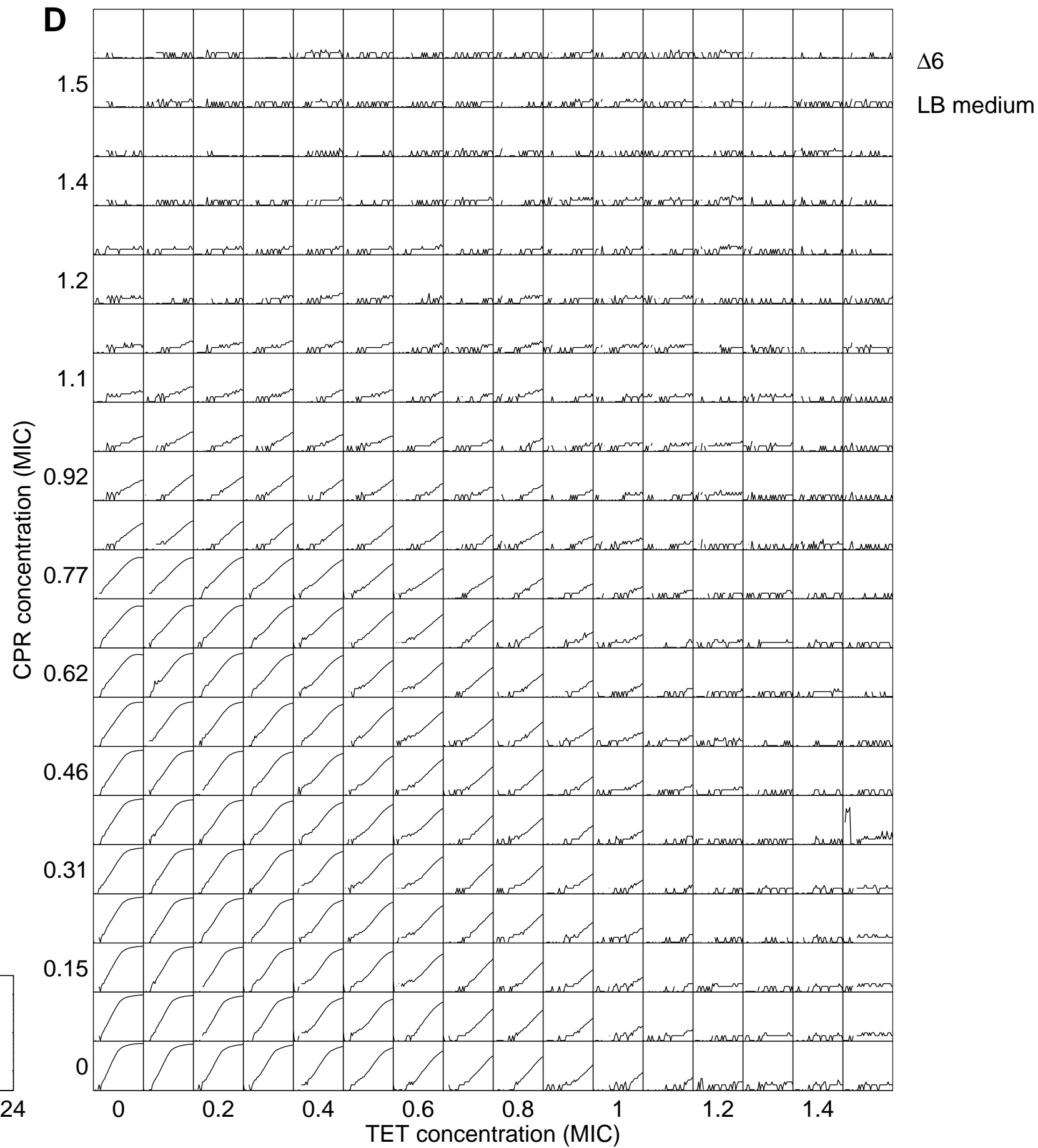


Figure S9

**D**



**A**

WT MG1655  
LB medium

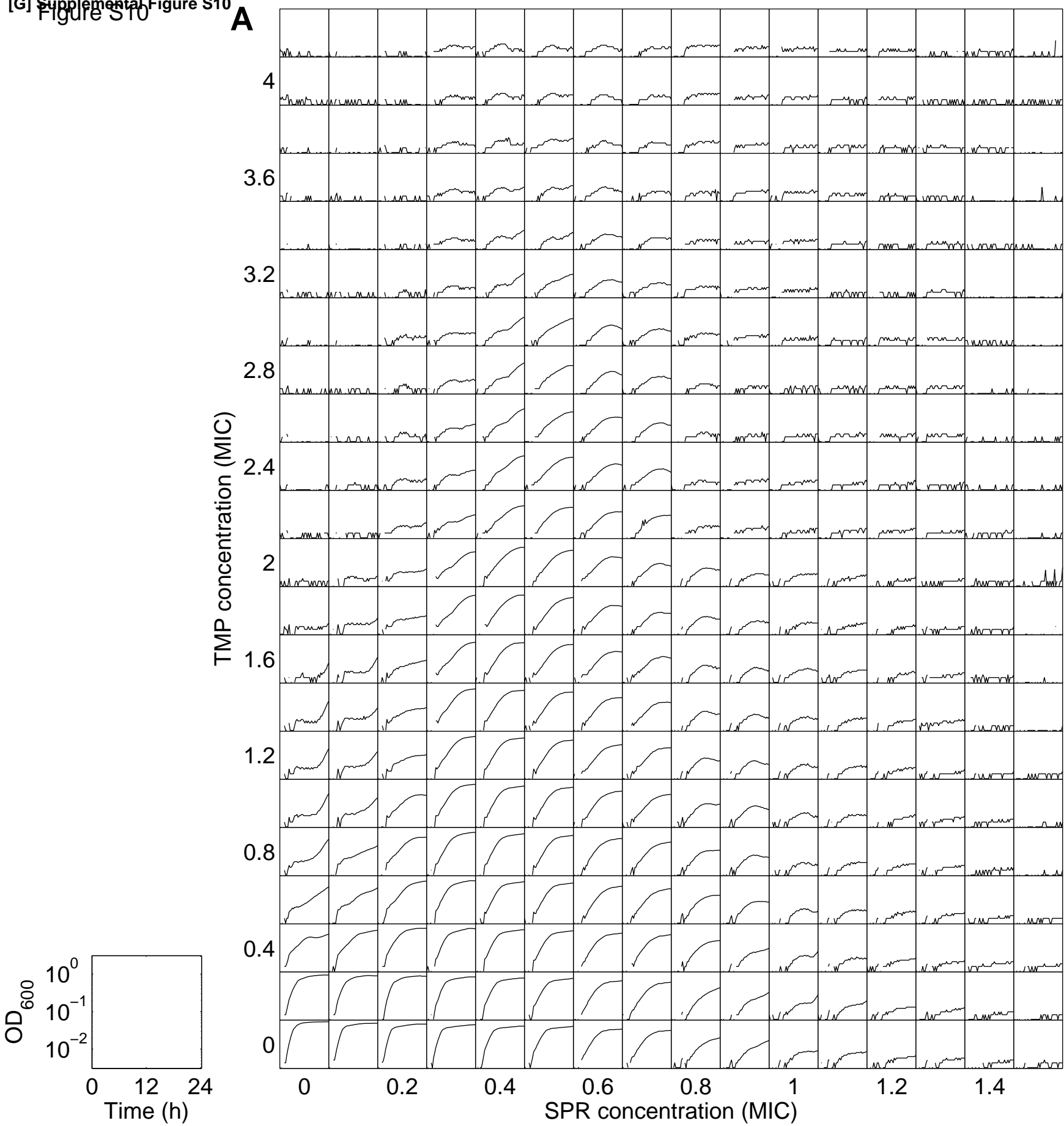


Figure S10

**B**

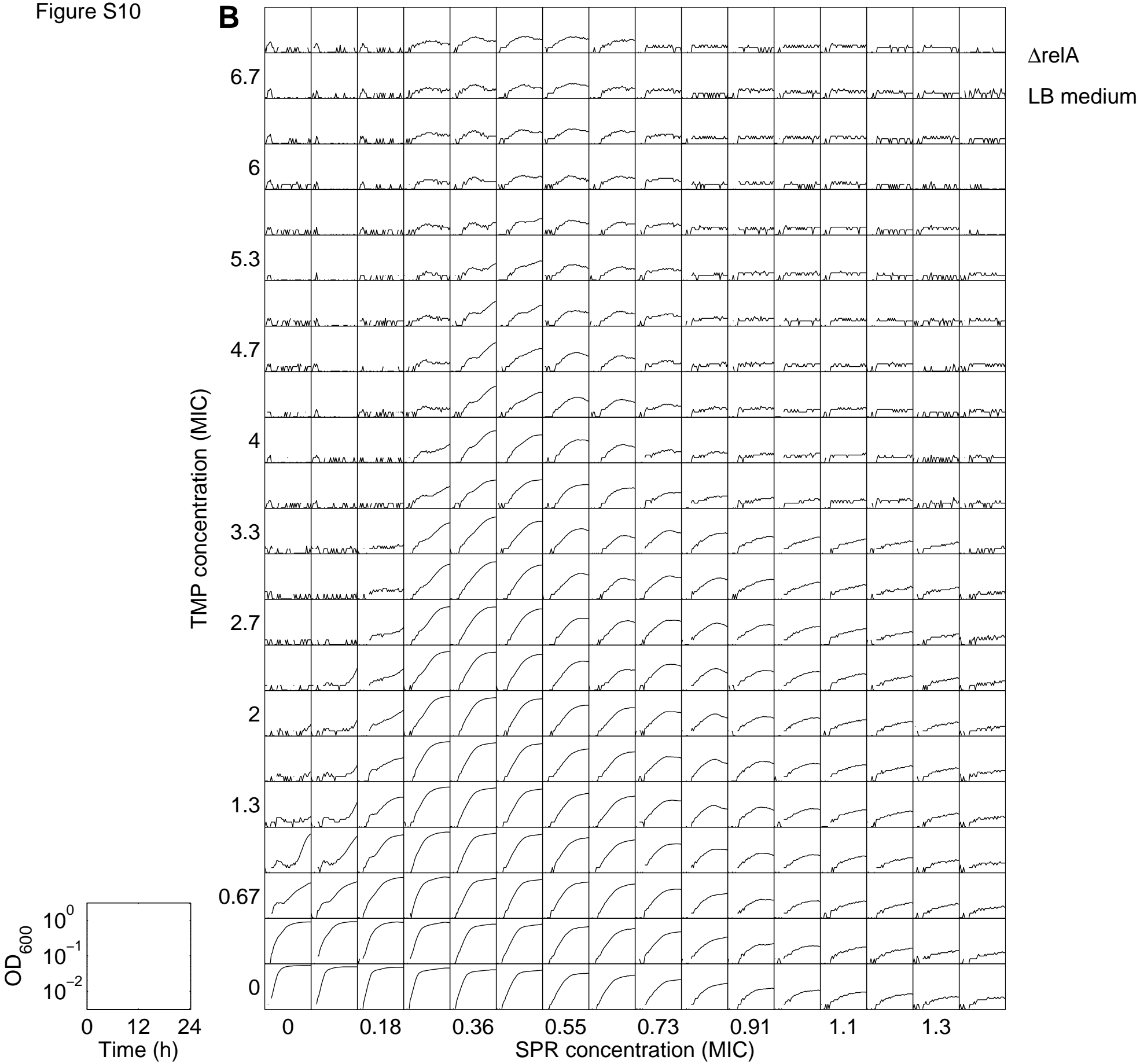


Figure S10

